International Journal of Earth Sciences (2025) 114:1051–1071
https://doi.org/10.1007/s00531-025-02532-z

ORIGINAL PAPER

U–Pb–Hf isotope and shape systematics of detrital zircon populations from the Badenweiler–Lenzkirch Zone, Black Forest (Germany): new constraints on sediment deposition, provenance and Variscan evolution

A. Zeh[1] · **M. Hinderer**[2] · **C. Diehl**[1] · **A. Gerdes**[3]

Received: 21 June 2025 / Accepted: 28 July 2025 / Published online: 5 August 2025

Abstract
Presently, little is known about the provenance and depositional ages of clastic metasedimentary rocks of the Badenweiler–Lenzkirch Zone (BLZ), which is squeezed between high-grade gneisses of the Central and Southern Black Forest Gneiss complexes. This lack of knowledge prevents detailed correlations with other sedimentary units and limits our understanding of the pre- to syn-Variscan evolution in Central Europe. In this study, we present the first set of data combining U–Pb ages, Hf isotope data, and shape parameters of detrital zircon populations of nine samples collected from three formations of the BLZ: Sengalenkopfschist, Schleifenbachschist, and Protocanites Greywacke. Based on biostratigraphic record, these formations are assumed to be deposited from the Early Ordovician to Early Carboniferous. This interpretation, however, is at odds with the detrital zircon age record, revealing robust maximum depositional ages between 368 and 378 Ma for all three units. Age spectra show peaks at 380–400 Ma, 480–500 Ma, 600–620 Ma, 700–750 Ma, 0.9–1.1 Ga, 1.8–2.2 Ga, and 2.6 Ga, and Hf isotopes a juvenile input at 380–410 Ma (εHf_t up to + 5). Combined zircon age-Hf isotope data point to three major sources, which are similar to the metamorphic gneiss units exposed in southern Black Forest (Wiese-Wehra, Todtmoos, and Murgtal), hosting relics of different Gondwana-derived terranes, in addition to a Late Devonian arc-back arc system. The finding of abundant zircon grains of euhedral shape in all BLZ samples and similar zircon typologies additionally suggest supply from a proximal magmatic arc source.

Keywords Black Forest · Zircon · U–Pb-dating · Hf isotopes · Shapes · Provenance

Introduction

The Black Forest (Schwarzwald) in southern Germany forms a central part of the Variscan Orogen (Fig. 1a), which is interpreted to result from the amalgamation of several microcontinents and terranes, and closure of oceanic basins in between (e.g., Stampfli et al. 2002; von Raumer et al. 2002, 2013; Franke et al. 2017; Neubauer et al. 2022). These microcontinents were originally located along the northern margin of Gondwana until ca. 500 Ma, and underwent a differential drift history until 350 Ma (e.g., Tait et al. 1997; Linnemann et al. 2000; Zeh et al. 2001, 2023; Žák et al. 2023). Some authors argue that all Variscan terranes have been assembled within an extremely wide shelf that never left mainland Gondwana until the Variscan collision (e.g., Linnemann et al. 2004; Kroner and Romer 2013; Žak and Sláma 2017; Žák et al. 2023), whereas other authors suggest a proper rift history, with the formation of oceanic realms between individual terranes (e.g., Haas et al. 2020; Finger and Riegler 2022; Neubauer et al. 2022; Zeh et al. 2023). In the Black Forest, the Paleozoic drift history is assumed to be preserved in the low-grade metasedimentary rocks of Badenweiler–Lenzkirch Zone (BLZ), which forms a ca. 5 km wide

✉ A. Zeh
armin.zeh@kit.edu

[1] Institute for Applied Geosciences, Mineralogy and Petrology, KIT - Karlsruhe Institute of Technology, Adenauerring 20B, Geb. 50.4, 76131 Karlsruhe, Germany

[2] Institute of Applied Geosciences, Technical University of Darmstadt, Schnittspahnstr. 9, 64287 Darmstadt, Germany

[3] Frankfurt Isotope and Element Research Center (FIERCE), Goethe-University Frankfurt, 60438 Frankfurt am Main, Germany

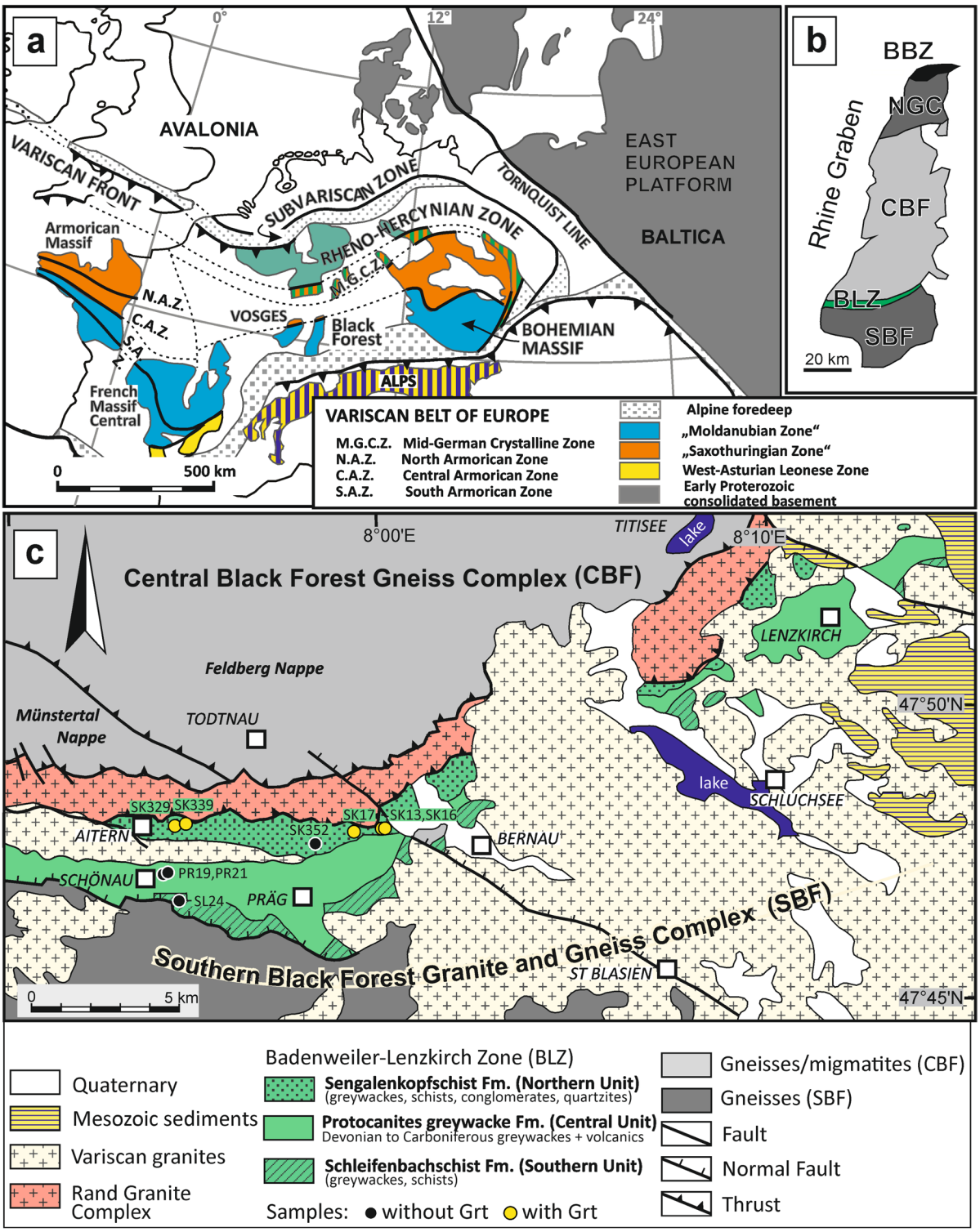

Fig. 1 **a** Position of the Black Forest in the Moldanubian Zone of the European Variscan Belt (modified after Schönenberg and Neugebauer 1997). **b** Geological Units of the Black Forest Gneiss Complex: *BBZ* Baden-Baden Zone, *NGC* Northern Granite Complex with gneiss slivers, *CBF* Central Black Forest Gneiss Complex, *BLZ* Badenweiler-Lenzkirch Zone, *SBF* Southern Black Forest Gneiss Complex. **c** Geological map of the Zone of Badenweiler-Lenzkirch (modified after Sawatzki and Hann 2003)

belt squeezed between high-grade gneisses of the Central and Southern Black Forest gneiss complexes (Fig. 1b). Previous studies suggest that the protoliths of the BLZ metasediments, mostly shales and greywackes, were deposited in a deep marine basin between the Early Ordovician and Early Carboniferous. This interpretation is supported by the biostratigraphic record, comprising goniatites, conodonts, acritarchs, and chitinozoans, which have rarely been found in schist and greywacke layers (Weyer 1962; Kneidel et al. 1982; Hann et al. 1995; Güldenpfennig 1997; Montenari et al. 2000; Vaida et al. 2004; Korn and Montenari 2023). Metarhyolithic layers yielded a lower Devonian age at 393 Ma (Pb-Pb zircon evaporation: Hann et al. 2003a), whereas metaconglomerates, locally associated with the greywackes, were interpreted to represent diamictites related to the Hirnantian glaciation of Gondwana (Ziegler and Wimmenauer 2001). Presently it remains unknown whether the BLZ sediments result from a continuous deposition from the Early Ordovician to the Early Carboniferous, or from periodic input. Furthermore, nearly nothing is known about the provenance of the clastic sedimentary rocks, and the magmatic evolution in the pre-Variscan hinterland. Based on Pb-Pb ages of 16 detrital zircon grains along with bulk-rock (isotope) geochemical data, Hegner et al. (2005) postulated a provenance located to the north of the BLZ, although barely supported by the geological record.

To place new constraints on the evolution of the Variscan basement exposed in the southern part of the Black Forest, we present in this study a comprehensive set of data, comprising U–Pb ages, Hf isotope data, and shape parameters of detrital zircon populations from nine samples of different units of the BLZ. These data, along with compilations, will place new constraints on maximum depositional ages, sediment provenance and transport, as well as on the pre- to syn-Variscan crustal evolution in the hinterland. Furthermore, significant inconsistencies will be revealed between the biostratigraphic record and detrital zircon ages, which require significant revisions of previous concepts. Finally, a model is presented, which provides new insight into the pre- to syn-Variscan evolution of the Moldanubian realm in Central Europe prior to 370 Ma.

Geological setting of the Black Forest

The Black Forest (Schwarzwald) in southern Germany forms a ca. 2000 km^2 basement complex of the Variscan Belt (Fig. 1). Based on detailed mapping, the basement is subdivided into five major units, which are designated from north to south as: (1) Baden-Baden Zone, (2) Northern Black Forest Granite Complex, (3) Central Black Forest Gneiss Complex, (4) Badenweiler–Lenzkirch Zone (BLZ), and (5) Southern Black Forest Gneiss Complex (Fig. 1b). While the Northern Black Forest Granite Complex is dominated by Variscan granites, the other four units mainly consist of metasedimentary rocks of presumably Neoproterozoic to Palaeozoic age (Wimmenauer 1988; Montenari et al. 2000; Hanel et al. 2001; Vaida et al. 2004; Zeh et al. 2023), but were affected by a different degree of metamorphic overprint, from greenschist to eclogite- and granulite-facies during the Variscan orogeny (e.g., Kalt et al. 2000; Marschall et al. 2003). Locally, these units contain pre-Variscan orthogneisses of Cambrian age (e.g., Chen et al. 2000), and were intruded by late Variscan granites at 340–335 Ma (for summary see Kroner et al. 2008).

The **Baden-Baden Zone** is traditionally considered to be part of the Saxothuringian Zone of the Variscan Belt, and the four southern units part of the Moldanubian Zone after Kossmat (1927). The Baden-Baden Zone consists of greenschist to amphibolite-facies metamorphic rocks, mostly metagreywackes, quartzites, carbonate rocks intercalated by mafic volcanic rocks (diabase). This assembly of rocks is interpreted to represent accreted crustal fragments with different metamorphic and tectonic histories (Wickert et al. 1990; Kalt et al. 2000). Acritarchs suggest an Upper Cambrian to Lower Ordovician depositional age (Montenari and Servais 2000).

The **Northern Black Forest Granite Complex** separates the low- to medium-grade metamorphic rocks of the Baden-Baden Zone from the high-grade metamorphic gneisses of the Central Black Forest Gneiss Complex. The complex mainly consists of Variscan granites of different composition and origin (Altherr et al. 1999, 2000), which intruded into pre-Variscan ortho- and paragneisses mainly exposed in the Omerskopf area.

The **Central Black Forest Gneiss Complex** comprises a pile of nappes. It is interpreted as a bivergent "pop-up" structure that has been thrust together with gneisses of the Northern Black Forest Granite Complex over the Baden-Baden Zone to the north and the BLZ to the south (Eisbacher et al. 1989). Four nappes are distinguished, which are from top to the bottom: (1) the Feldberg Nappe, representing a monotonous gneiss unit with high-pressure relicts (unit 1 of Hanel and Wimmenauer 1990; Kalt and Altherr 1996), (2) the Granulite Nappe, consisting mainly of retrogressed granulites (unit 3 after Röhr 1990; Hanel et al. 1993), (3) the Münstertal Nappe, comprising a wide range of metamorphic rocks without any high-pressure relicts (unit 2 after Flöttmann and Kleinschmidt 1989; Hanel and Wimmenauer 1990), and (4) the Rand Granite Nappe (Hann et al. 2003b). The metamorphic rocks were intruded by Variscan granites at ca. 335–330 Ma, the largest of which is the Triberg Granite (e.g., Schleicher 1994).

The **BLZ**, which is the focus of this study, forms a small belt of low-grade sedimentary and volcanic rocks (ca. 40 km long and 5 km wide), separating the high-grade metamorphic rocks of the Central Black Forest Gneiss Complex from

the Southern Black Forest Gneiss Complex (Fig. 1b, c). The BLZ is interpreted as an E-W trending syncline, which was formed in a dextral transpressional regime during Variscan collision at ca. 340–330 Ma. It is limited to the north by sheared granitoid rocks of the Rand Granite Nappe (Hann et al. 2003b), with the youngest porphyritic granites dated at 330.9 ± 4.8 Ma (SIMS U–Pb zircon; Altherr et al. 2019). The BLZ is subdivided by the Stratigraphic Commission of Germany (Hanel et al. 2001) into three units designated as Sengalenkopfschist Formation (Northern Unit), Protocanites Greywacke Formation (Central Unit), and Schleifenbachschist Formation (Southern Unit; Fig. 1c). The two basal formations (Sengalenkopfschist and Schleifenbachschist) consist of low- to medium-grade phyllites, metasiltstones, metagreywackes, metaconglomerates, and quartzites, which are suggested to be deposited in marine environments during the Ordovician to Silurian/Early Devonian (Hann et al. 1995; Montenari et al. 2000; Vaida et al. 2004). Vaida et al. (2004) subdivided the Sengalenkopfschist Formation further into two belts: a southern belt of Early Ordovician age (late Arenig to earliest Llanvirn) dominated by metagreywackes and metapelites (Typ Aitern after Güldenpfennig 1997), and a northern belt of Silurian (Wenlock to Ludlow) to early Devonian age dominated by metasiltstones with some metarhyolitic lenses, layers, and locally decameter size bodies around Präg or at the top of the Säuling. Three zircon grains of one metarhyolith layer from the Sengalenkopf-Prägbach zone were dated by Pb-Pb evaporation technique at 393 Ma (Hann et al. 2003a). Poorly preserved chitinozoans found in the Schleifenbachschist Formation are not diagnostic and limit the age of sediment deposition roughly between Ordovician and Early Devonian (Fig. 2). Metaconglomerates of the Sengalenkopfschist Formation were interpreted as dropstones formed during the Ordovician (Hirnantian) glaciation of Gondwana (Ziegler and Wimmenauer 2001). The two basal units of the BLZ are overlain by a (meta) greywacke sequence (Protocanites Greywacke Formation) of Tournaisian age, as inferred from goniatites (Korn and Montenari 2023). Conodonts locally found in marine shale lenses indicate a Late Devonian age (Weyer 1962; Kneidel et al. 1982). The Protocanites greywacke sequence is crosscut by rhyodacite dikes and overlain by pyroclastic rocks of Viséan age (340 ± 2 Ma, U–Pb zircon TIMS dating; Schaltegger 2000). Finally, the basement units of the BLZ are intruded by Variscan granites (Münsterhalden, Sankt Blasien, Bärhalde granite) at 333 ± 2 Ma (U–Pb TIMS: Schaltegger 2000) and covered by molasse-type sediments (Badenweiler Conglomerate Formation) of Late Viséan age (Fig. 2).

The **Southern Black Forest Gneiss Complex** is subdivided by the Stratigraphic Commission of Germany (Hanel et al. 2001) into three major units: (1) Murgtal, (2) Todtmoos, and (3) Wiese-Wehra Gneiss units, which underwent a Viséan high-T/low-P metamorphism. The Wiese-Wehra unit is interpreted to form a nappe (Hann and Sawatzki 1998), which has been thrust above the other two gneiss units under ductile conditions between 342 and 333 Ma (Hegner et al. 2001), followed by the intrusion of Variscan granites at 334 ± 3 Ma (e.g., Albtal granite: U–Pb-zircon ID-TIMS: Schaltegger 2000). Results of a recent provenance study indicate that the Murgtal unit hosts the oldest sedimentary rocks of the Southern Black Forest Gneiss Complex, i.e., greywackes of Ediacarian age deposited at < 545 Ma (Zeh et al. 2023), perhaps overlain by Cambro-Ordovician to Silurian sedimentary sequences, as concluded from acritarchs and chitinozoans in graphite-rich (meta)sedimentary rocks (Vaida et al. 2004). Sedimentary protoliths of the Wiese-Wehra and Todtmoos Gneiss units were deposited during the late Devonian at < 375 Ma in different geotectonic settings (Fig. 2). The Wiese-Wehra metagreywackes host relics of a Cadomian oceanic arc formed at 610 Ma ($\varepsilon Hf_t = +5$ to $+8$), but also of a Late Devonian-Early Carboniferous arc-back arc system with juvenile input at ca. 375 Ma ($\varepsilon Hf_t = 0$ to $+10$; Zeh et al. 2023). A juvenile arc setting is also reflected by relics of a mafic layered intrusion (Sebert and Wimmenauer 1992), which emplaced the Wiese-Wehra unit at ca. 350 Ma ($\varepsilon Nd_t = 6.3$; Hegner et al. 2001). Detrital zircon grains in Todtmoos metaarkoses reflect subduction-related magmatism at 490–420 Ma, and at 380 Ma in a continental arc setting ($\varepsilon Hf_t = -2$ to -8; Zeh et al. 2023).

Samples

During this study, zircon populations from nine (meta) sedimentary rock samples of the BLZ were investigated for U–Pb dating and zircon shape analyses. Three of these samples were additionally analysed for Lu–Hf isotopes. Two samples are from the Protocanites Greywacke Formation (PR19, PR21), one from the Schleifenbachschist Formation (SL24), and six samples from the Sengalenkopfschist Formation (SK13, SK16, SK17; SK329, SK339, SK352)—(for sample localities see Table 1 and Fig. 1c). The samples PR19 and PR21 are weakly deformed polymictic greywackes. Sample PR21 is coarse-grained with round clasts having sizes up to 5 mm in diameter (conglomerate), while the grains of sample PR19 are mostly < 2 mm (sand fraction). The detritus in both samples is dominated by lithic clasts, mainly felsic volcanic rocks (K-feldspar and/or quartz phenocrysts setting in a fine grained or glassy-recrystallized matrix), and minor metamorphic rocks (phyllites, quartz-phyllites). The lithic clasts are commonly embedded in a fine-grained "clayish" matrix consisting of sericite-chlorite, silty quartz, and feldspar clasts. The rocks of the Schleifenbachschist and Sengalenkopfschist formations are commonly well foliated, except quartzite sample SK16, which appears compact and is composed of re-crystallised undulatory quartz and minor plagioclase and garnet. Three samples

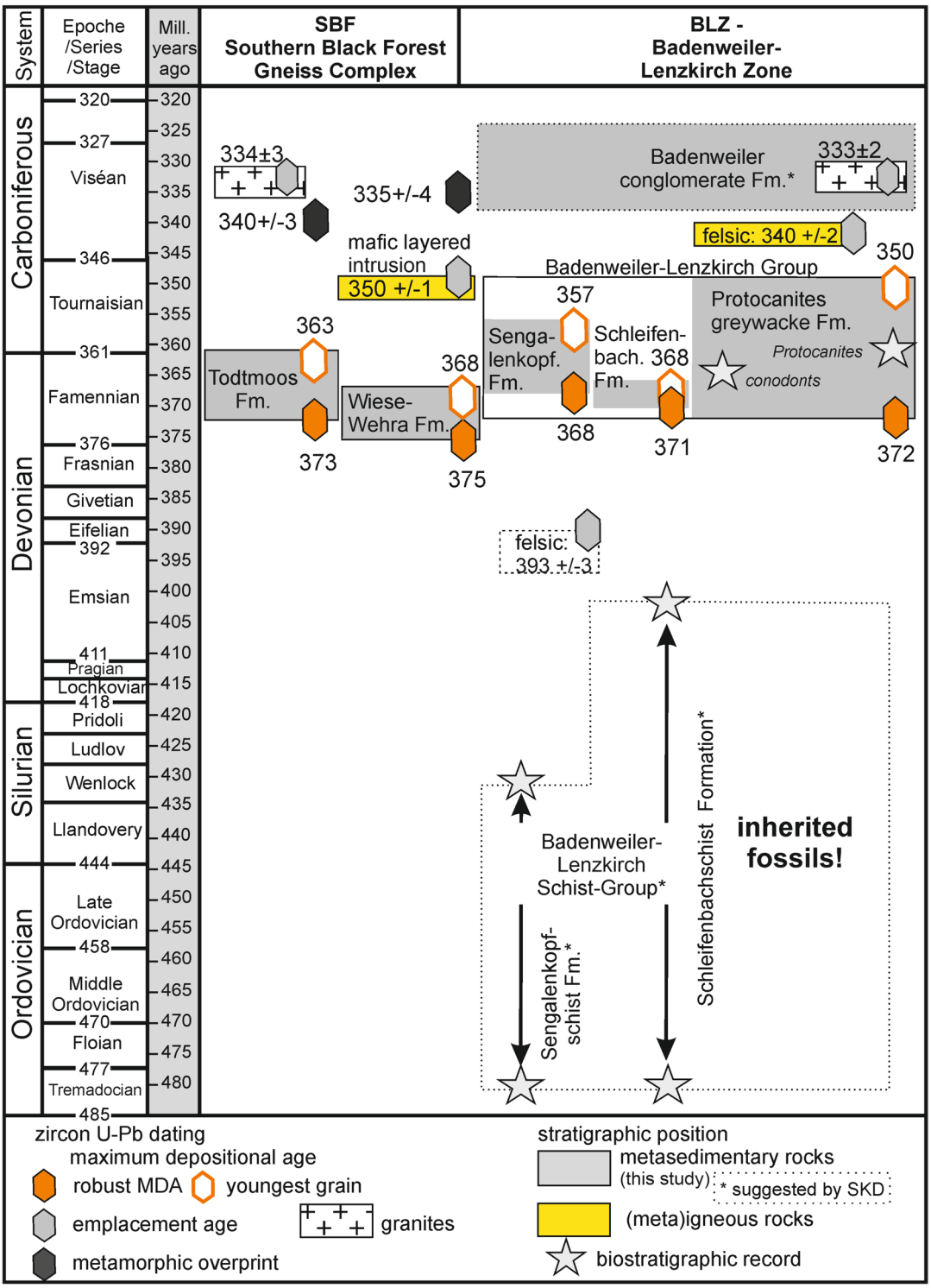

Fig. 2 Process-chronological table compiling zircon U–Pb ages and stratigraphic positions of metasedimentary rock units of the Southern Black Forest Gneiss Complex (SBF) and the Badenweiler-Lenzkirch Zone (BLZ). Data sources: zircon ages of SBF (Zeh et al. 2023), BLZ (this study), (meta)igneous felsic rocks (Hann et al. 2003a; Hegner et al. 2005), granites (Schaltegger 2000); Bio-lithostratigraphic record according to SKD (Stratigraphische Kommission Deutschland; Hanel et al. 2001) and data from Kneidl et al. (1982) and Vaida et al. (2004)

Table 1 Co-ordinates of rock samples from the Badenweiler–Lenzkirch zone

Sample	Rock type	Location	Sample co-ordinates	
			Longitude S	Latitude E
Protocanites greywacke unit (central unit)				
PR19	Metagreywacke (fine)	Wiese valley, at northern end of Schönau	47°46′51.97″	7°54′41.06″
PR21	Metagreywacke (coarse)	Wiese valley, at northern end of Schönau	47°46′51.97″	7°54′41.06″
Sengalenkopfschist unit (northern unit)				
SK13	Metagreywacke (banded), Grt	Quarry "Wacht" at road L149 near Bernau	47°48′16.59″	8°00′19.08″
SK16	Impure quartzite, Grt	Quarry "Wacht" at road L149 near Bernau	47°48′16.59″	8°00′19.08″
SK17	Metaconglomerate, C, Grt	Road L149 Bernau-Präg (small trail)	47°48′14.38″	7°59′18.30″
SK329-5	Metaconglomerate, C, Grt	Utzenfeld	47°79′83.63″	7°97′31.57″
SK339-P	Metagreywacke (fine), C	Utzenfeld	47°80′29.79″	7°92′23.36″
SK352-M	Metagreywacke, Grt	Sengalenkopf	47°80′49.57″	7°92′79.30″
Schleifenbachschist unit (southern unit)				
SL24	Metagreywacke (schistous), C	Road Schönau to Tunau	47°46′57.91″	7°54′30.17″

C—graphite-bearing, Grt—garnet-bearing

of the Sengalenkopfschist Formation are from localities previously investigated for acritarchs and chitinozoans by Vaida et al. (2004); (1) sample SK339: fine-grained metagreywacke from Utzenfeld (close to sample #1 of Vaida et al. 2004; suggested biostratigraphic age: Early Ordovician); (2) sample SK352: metasiltstone/phyllite from the Sengalenkopf area (close to sample #45 of Vaida et al. 2004; suggested biostratigraphic age: Silurian; (3) sample SK329: metaconglomerate from the Sengalenkopf area; previously interpreted by Ziegler and Wimmenauer (2001) to represent a "dropstone" deposit of Hirnantian age. The other three samples (SK13: metagreywacke; SK16: quartzite; SK17: metaconglomerate) are either from the quarry "Wacht" near Bernau (close to the location sampled by Hann et al. (2003a) for metarhyolith dating) or ca. 1 km east of it (Fig. 1c). These samples are from the "Silurian northern belt" defined by Vaida et al. (2004). All samples of the Sengalenkopfschist Formation, except SK352 (from Utzenfeld) contain euhedral garnet porphyroblasts up to 200 µm in diameter, found in heavy mineral concentrates.

Analytical methods

Zircon separation and imaging

Representative zircon populations were recovered from nine samples of ca. 1 kg weight. The samples were crushed with a jaw crusher (< 3 mm) and steel disc mill to grain sizes < 500 µm (2 min in disc mill), and the heavy mineral fraction was enriched by panning only. Finally, zircon grains were manually selected with a brush from the panning concentrates under ethanol. To select a representative population, ca. 200 grains per sample were systematically picked after multiple steerings (homogenization) the concentrate for about 1 min with a brush. Subsequently, all grains were selected from (sub)aliquots, independent of size, shape, and degree of alteration or fracturing. The selected populations were pipetted with ethanol on double-sided tape, sputtered with Au for 15 s, and imaged for their morphologies by backscattered electron (BSE) microscopy using a TESCAN VEGA2 scanning electron microscope at the Department of Mineralogy and Petrology at Karlsruhe Institute of Technology (KIT). Representative images are shown in Fig. 3. Subsequently, the same grains were mounted with epoxy and ground to expose their centre parts. The polished grains were imaged again by BSE to gain information about their internal zoning. Subsequently, each grain was numbered, and the populations were investigated for zircon shape (all selected grains per sample), U–Th–Pb dating (120–150 grains per sample) and Hf isotope analyses (70 grains per sample; selected based on the results of U–Pb dating; only grains with concordance level 90–110%).

Zircon U-Th-Pb analyses

Uranium-Th-Pb analyses were performed by laser ablation— sector field—inductively coupled plasma mass spectrometry (LA-SF-ICP-MS) during 4 sessions, using a 193 nm ArF Excimer laser (Analyte Excite +, Teledyne Photon Machines) coupled to a Thermo-Scientific Element XR instrument at KIT, Karlsruhe, Germany. Zircon grains of unknown age were analysed together with the

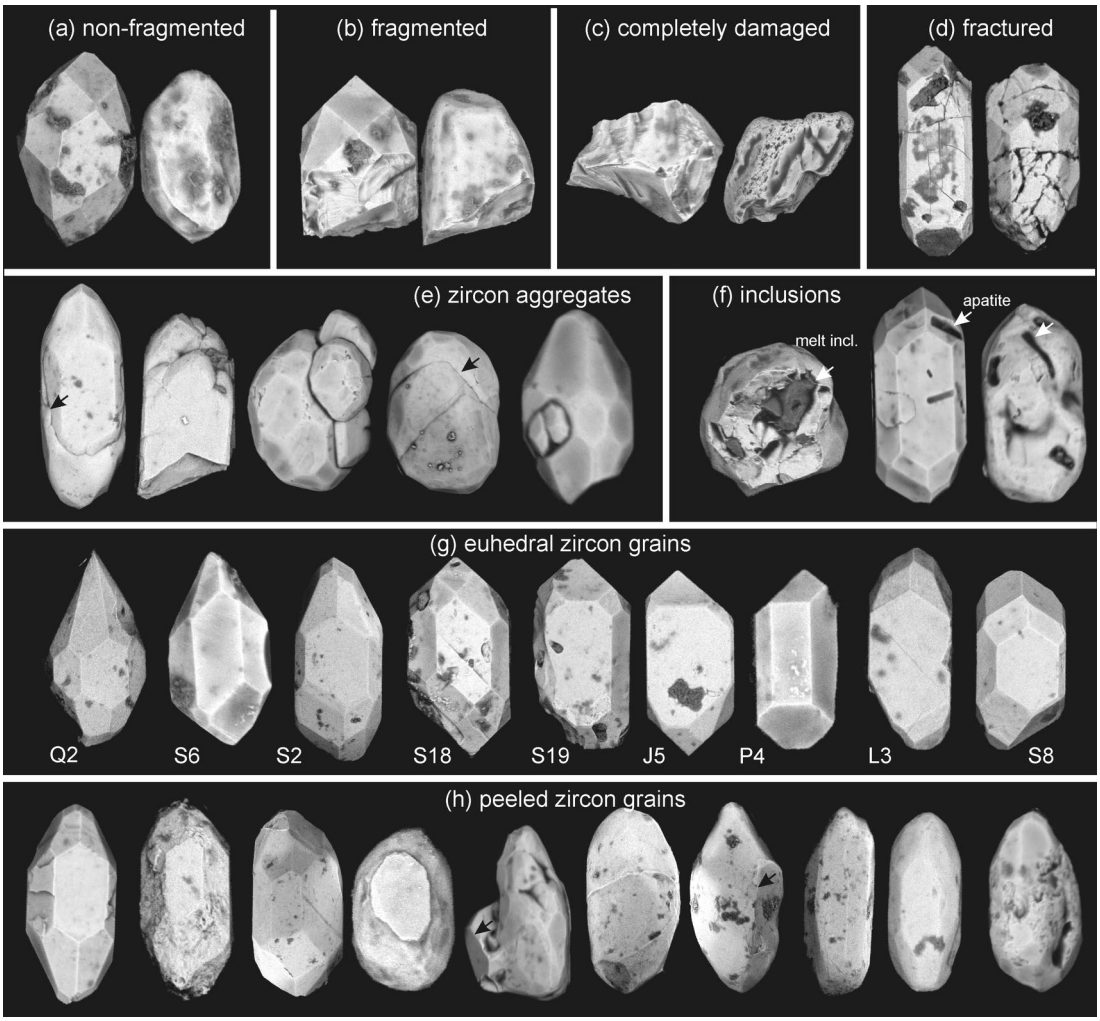

Fig. 3 Representative images of zircon grains found in metagreywackes of the Badenweiler-Lenzkirch Zone. **a-d** non-fragmented, fragmented, completely damaged, and fractured zircon grains. **e** zircon grain aggregates, **f** zircon grains with apatite and melt inclusions, **g** zircon crystals of perfect euhedral shape with different typologies (typology classification Q2, J2, etc. according to Pupin 1980), **h** zircon grains disintegrated by peeling (removal of the outer shell) during sediment transport and/or metamorphic overprint

reference zircon BB (primary standard), Plešovice, and KA1 (KaapValley), using a laser spot diameter of 20 µm, a laser fluence of 2.7 Jcm^{-2}, at a 10 Hz repetition rate, RF power = 1230 W, a mixed Ar-He-N_2 carrier gas consisting of Ar = 0.91 $Lmin^{-1}$, He = 0.3 cell + 0.2 cup (both $Lmin^{-1}$), and N_2 = 0.0012 $Lmin^{-1}$. Three pulses of pre-ablation were obtained prior to each analysis of 15 s duration following a 15 s background measurement. All raw data were corrected offline using an in-house MS Excel© spreadsheet program (Gerdes and Zeh 2006, 2009). A common Pb correction based on the interference and background corrected ^{204}Pb signal and a model Pb composition were applied (Stacey and Kramers 1975). More detailed information about analytical conditions are presented in ESM (Table S1), and the results of measurements of reference zircons and unknowns in ESM (Table S2). The results of U–Pb dating are summarized in Table 2. Concordia diagrams were plotted by means of the software ISOPLOT 3.75 (Ludwig 2012), and age spectra with the freeware AgeDisplay (Sircombe 2004), using $^{206}Pb/^{238}U$ ages for analyses with ages < 1000 Ma, and $^{207}Pb/^{206}Pb$ ages of all zircon analyses with ages > 1000 Ma, and with a concordance level of 90–110% (Fig. 4a).

Lu–Hf isotope analyses

Lutetium–Hf isotope analysis was carried out with a Resolution M-50 193 nm ArF Excimer laser system coupled to a Thermo-Scientific multicollector (MC)-SF-ICP-MS (Neptune Plus) at FIERCE Frankfurt am Main, Germany. The analytical protocols used are the same as described in detail by Gerdes and Zeh (2006). Detailed operating conditions for Lu–Hf isotope analyses and results of standard

Table 2 Results of U–Pb zircon dating

Sample	n[a]	n[b]	%	MDA[c]	±2σ	RMDA[d]	±2σ	$MSWD_{CE}$	$Prob_{CE}$	n[e]
	(all)	(90–110%)		(Ma)		(Ma)				
Protocanites greywacke unit (central unit)										
PR19	119	87	73	365	6	**372.1**	**2.5**	1.70	0.10	14
PR21	150	102	68	350	6	**373.3**	**2.4**	1.00	0.45	8
Sengalenkopfschist unit (northern unit)										
SK13	120	89	74	367	6	**371.2**	**1.8**	1.12	0.30	14
SK16	117	91	76	357	6	**372.1**	**1.9**	0.78	0.81	16
SK17	119	86	72	358	6	**368.0**	**2.2**	1.30	0.13	12
SK329-5	119	91	76	366	9	**376.7**	**2.0**	1.16	0.23	20
SK339-P	120	94	78	378	11	**378.3**	**3.7**	0.36	0.98	7
SK352-M	125	94	75	368	9	**378.0**	**2.1**	1.10	0.30	21
Schleifenbachschist unit (southern unit)										
SL24	149	104	70	367	10	**370.6**	**2.2**	1.20	0.18	14

a—number of all analyses per sample

b—number of analyses with concordance level 90–110%

c—MDA—maximum depositional age defined by youngest zircon grain of 100% concordance

d—RMDA—robust maximum depositional age defined by youngest zircon age cluster (bold ages are most reliable)

e—number of grains used for RMDA calculation

$MSWD_{CE}$ -Mean Square Weighted Deviation (of concordance and equivalence)

$Prob_{CE}$—Probability (of concordance and equivalence)

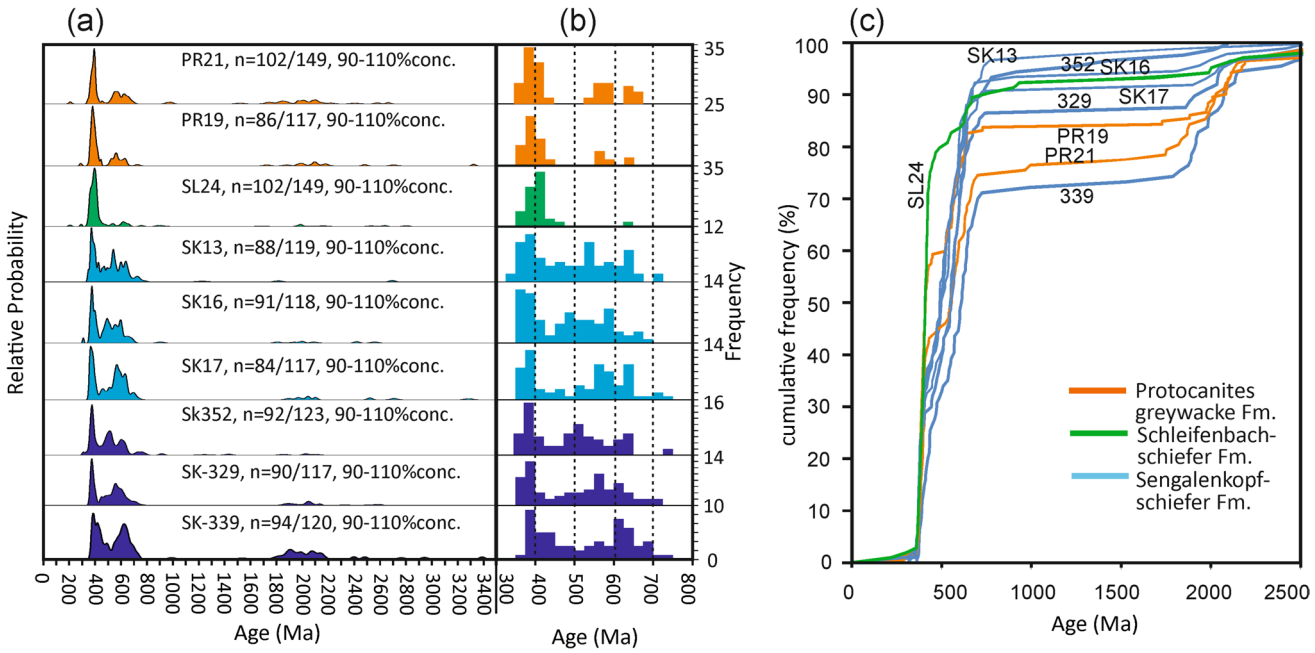

Fig. 4 Age spectra of zircon populations in metasedimentary rocks of the three formations (SK-Sengalenkopfschist, PR-Protocanites Greywacke, SK-Schleifenkopfschist) of the Badenweiler-Lenzkirch Zone. **a** Age vs. relative probability diagrams, **b** Age vs. frequency diagrams, **c** Age vs. cumulative frequency diagram

measurements are presented in ESM (Table S3). Multiple measurements of reference zircon GJ1 and Temora-1 during the analytical session yielded $^{176}Hf/^{177}Hf$ ratios of 0.282000 ± 0.000026 (2σ S.D.) and 0.282650 ± 0.000031

(2σ S.D.) respectively, in agreement with published values (Woodhead and Hergt 2005).

For calculation of the epsilon Hf (εHf_t), the chondritic uniform reservoir (CHUR) was used as recommended by Bouvier et al. (2008); $^{176}Lu/^{177}Hf$ and $^{176}Hf/^{177}Hf$ of 0.0336 and 0.282785, respectively, and a decay constant of 1.867×10^{-11} (Scherer et al. 2001; Söderlund et al. 2004). Two-stage Hf model ages (T_{DM}) were calculated by applying $^{176}Hf/^{177}Hf = 0.283181 \pm 0.00023$ ($n = 46$) and $^{176}Lu/^{177}Hf = 0.038055$ for the depleted mantle (DM) evolutionary line (average MORB composition of Atlantic and Indian oceans of Chauvel and Blichert-Toft 2001), resulting in a depleted mantle (DM) evolutionary line ranging from + 14 (today) to zero (at 4.56 Ga). Crustal evolutionary trends were modelled by applying $^{176}Lu/^{177}Hf = 0.0113$ for continental crust (average of Taylor and McLennan 1985 and Wedepohl 1995). For all detrital zircon grains, initial $^{176}Hf/^{177}Hf$, εHf_t and T_{DM} were calculated using the $^{207}Pb/^{206}Pb$ ages obtained for the respective zircon domains (ESM: Table S3).

Zircon shape parameters and alpha decay doses

Shape parameters of zircon grains (length, width, aspect ratios, roundness and typologies) were quantified using BSE images. Length and aspect ratios were only obtained from non-fragmented grains, and the width parameter from all suitable fragments. The degree of roundness (DOR) was estimated by applying the classification scheme of Zeh and Cabral (2021), which distinguishes five classes: (1) all zircon edges are perfectly angular, (2) most/all edges are slightly rounded, (3) most edges and tips are significantly rounded, but the typology can still be classified by applying the classification scheme of Pupin (1980), (4) all edges and tips are strongly rounded, but faces are relic preserved, (5) completely rounded grains, without any primary faces. Zircon typologies were classified using the classification scheme of Pupin (1980) for all zircon grains with DOR = 1–3, including fragments having a sufficient number of faces allowing an unambiguous identification. The average temperatures were calculated according to Pupin (1980) as following: $avT = \sum_{i=600}^{900} n_i T_i$ (for $i = 600$, 650, 700, 750, 800, 850, 900°C), and alpha-decay doses by applying the equations of Murakami et al. (1991), using the U and Th contents analysed by LA-ICP-MS. The results are presented in ESM (Table S4), and summarized in Table 3.

Statistical data comparison

Statistical comparison of age spectra (1D), and combined age-εHf_t data (2D) were carried out with the R-freeware "detzrcr" of Andersen et al. (2018), using an age-bandwidth of 30 Ma, εHf_t-bandwidth of 2.0, and only age data with a concordance level of 90–110%. Agreement between age spectra (translated into cumulative probability; see Fig. 4b) is evaluated on the basis of two parameters: (1) "likeness" value of Satkoski et al. (2013), and (2) "0–1" parameter of Andersen et al. (2018). High agreement is commonly reflected by "likeness" values > 0.70, and "0–1" parameter 0.00–0.01 (for details see Andersen et al. (2018). The results are presented in Fig. 5.

Results

Zircon U–Pb ages

From each sample 120–150 zircon grains were systematically analyzed for U–Pb dating (ESM -Table S2). Care was taken to avoid fractures or altered domains (based on BSE images). Most of the analyses yield ages with concordance level 90–110% (68–78% per sample). These are the ones used for interpretation.

The zircon age spectra of the nine investigated samples show significant overlap but also differences, as is reflected by the data plotted in probability density and cumulative frequency diagrams (Fig. 4), as well as by significant variations in "likeness-values" (0.47 to 0.91), and "0–1 values" (0.00 to 0.05) presented in Fig. 5a. All samples show a pronounced age peak at 380–400 Ma, and the youngest concordant analyses (98–102%) yield Late Devonian—Early Carboniferous ages between 378 ± 11 and 350 ± 6 Ma. Robust maximum depositional ages based on the youngest age clusters range from 378.3 ± 3.7 to 368.0 ± 2.2 Ma (Fig. 6; Table 2).

All six SK samples from the Sengalenkopfschist Formation, independent of location or composition, show very similar age spectra ("likeness value" 0.70–0.91; except SK339), characterized by three age clusters: Paleozoic–Neoproterozoic (375–750 Ma; with peaks at 380–400 Ma, 480–500 Ma, 550–570 Ma, 600–620 Ma, 700–750 Ma), Paleoproterozoic (1.8–2.5 Ga), and Archean (2.5–3.4 Ga). The amount of zircon grains with Paleoproterozoic to Archean ages is variable among the samples. Such grains are most abundant in sample SK339 (ca. 30%) and 5–15% in all other samples. The age spectra of the SK samples significantly overlap those of the PR samples (Protocanites Greywacke Formation), as indicated by "likeness values" > 0.70. Although there is a clear difference in the Neoproterozoic age spectrum, which is significantly reduced in all PR samples, only revealing age peaks at 550–600 Ma and at ca. 650 Ma. The most simple age spectrum is reflected by sample SL24 (Schleifenkopfschist Formation), which is dominated by a single age peak at ca. 400 Ma, comprising ca. 80% of the analyses. Small peaks overlap those of the PR and SK samples. Zircon grains of Early Tonian–Stenian age (0.9–1.2 Ga) are very rare (< 3%)

Table 3 Results of zircon shape and U-Th analyses

Sample	PR19	PR21	SL24	SK13	SK16	SK17	SK352	SK339	SK329
No. of zircon shape analyses *n* =	223	208	196	200	223	180	167	195	182
Non-fragmented grains (%)	61	53	53	50	46	67	58	48	56
Shape parameters									
av. length (µm)	108	101	93	114	102	109	97	90	86
av. width (µm)	68	61	53	67	67	64	59	55	52
av. apect ratio	1.7	1.7	1.9	1.8	1.7	1.8	1.7	1.7	1.8
DOR—degree of roundness									
DOR 1 (%)	40	45	46	19	11	12	24	37	6
DOR 2 (%)	17	16	26	17	15	16	14	15	8
DOR 3 (%)	13	10	11	14	17	22	17	5	8
DOR 4 (%)	10	19	9	34	45	34	25	29	51
DOR 5 (%)	20	9	8	16	13	16	19	14	27
DOR (1 to 3)—(%)	*70*	*72*	*83*	*50*	*43*	*49*	*56*	*57*	*22*
av. DOR (#1)	*2.5*	*2.3*	*2.1*	*3.1*	*3.3*	*3.3*	*3.0*	*2.7*	*3.9*
Pupin parameter									
% of population (suitable)	53	55	65	39	31	43	47	43	19
av.T (°C)—(#2)	765	779	781	753	759	768	737	769	749
CSD—log normal (#3)									
no. of grains considered *n* =	207	183	180	181	189	174	161	174	172
N*	8	8	8	8	8	8	8	7	8
DF*	6	7	7	7	7	7	7	6	7
SL* (%)	> 20	> 20	10 to 20	> 20	< 1	> 20	> 20	> 20	> 20
$\chi 2$ value	5.9	4.3	9.9	4.1	45.2	5.5	5.7	4.5	4.6
no. U-Th analyses *n* =	119	150	149	120	117	119	125	120	119
U ppm (median)	428	344	489	312	266	220	218	266	285
Th ppm (median)	210	191	292	88	76	86	50	100	77
Th/U (median)	0.53	0.58	0.60	0.39	0.34	0.43	0.29	0.49	0.37

[#]1—average DOR = (1*DOR1%/100) + (2*DOR2%/100) + (3*DOR3%/100) + (4*DOR4%/100) + (5*DOR5%/100)

[#]2—calculated according toPupin (1980)

[#]3—CSD—crystal size distribution—log-normal (applied to width parameter)

parameters: *N** number of used channels (bins), *DF** degree of freedom, *SL** significance level of agreement, and $\chi 2$ value

(for more details see ESM-Fig.S1)

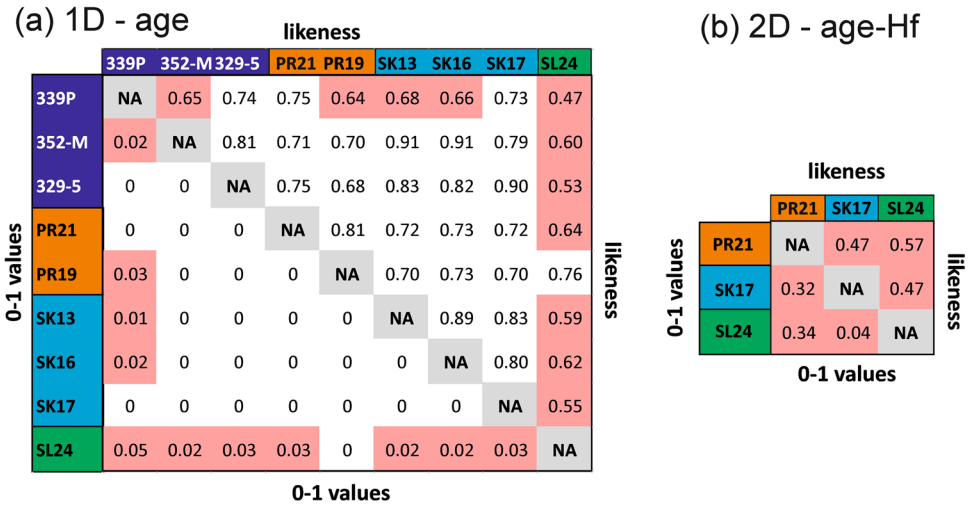

Fig. 5 Pairwise comparison of **a** zircon age spectra and **b** age-Hf isotope data of samples from the Badenweiler-Lenzkirch Zone. Numbers above NA-diagonal reflected "likeness" parameter (Satkoski et al. 2013), and beneath NA-diagonal "0–1" parameter (Andersen et al. 2018). The values were calculated with R freeware "detzrcr" (Andersen et al. 2018). High agreement is reflected by "likeness" value > 0.70 and "0–1" values 0.00–0.01

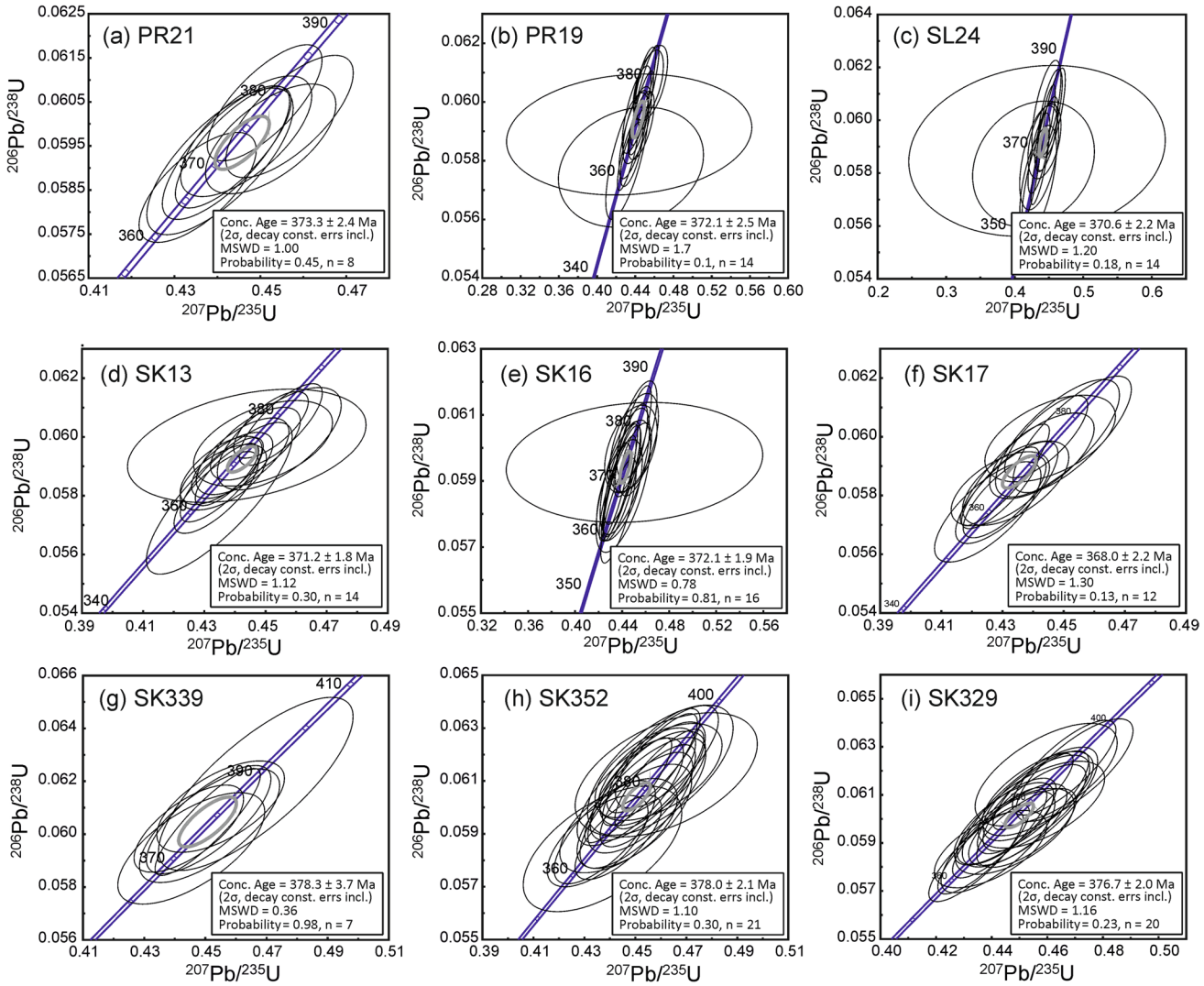

Fig. 6 Concordia diagrams showing robust maximum depositional ages for metasedimentary rocks of the Badenweiler-Lenzkirch Zone, derived from the youngest detrital zircon population

and were found sporadically in the samples PR21, SL24, SK13, SK16, SK329, SK339, SK16 (Fig. 4a).

Zircon Hf isotope analyses

Hafnium isotope analyses were only obtained from zircon grains of three samples (PR21: n = 70; SK17: $n = 70$; SL24: $n = 50$), one of each unit. The results are shown in Fig. 7 and ESM (Table S3). Zircon grains of different ages reveal significant variations in εHf_t values for all samples. Paleozoic zircon grains (350–539 Ma) show a wide scatter in εHf_t from + 13 to −15, which is mainly reflected by analyses of sample SK17. Most zircon grains of sample PR21 and SL24 (95%), and 40% of sample SK17 form a cluster with superchondritic εHf_t values between + 1 and + 5 at 370–420 Ma. Neo-Mesoproterozoic zircon populations (540–1100 Ma) reveal a wide scatter in εHf_t from + 15 to −29, Paleoproterozoic populations (1680–2400 Ma) from + 8 to −20, and Archean grains (2500–3400 Ma) from 0 to −10. We note that the overlap of combined age-εHf_t data among the three investigated samples is relatively poor, as indicated by "likeness-values" < 0.57, and "0–1 values" > 0.04 (Fig. 5b). Nonetheless, a similar source for all samples is indicated by the superchondritic age-εHf_t cluster at 370–410 Ma (Fig. 7b).

Zircon shape and physical parameters

In the investigated samples, zircon grains with a wide range in shapes and typologies have been observed, comprising non-fragmented, fragmented, and completely damaged grains (Fig. 3a–c), in addition to crystals of euhedral shape,

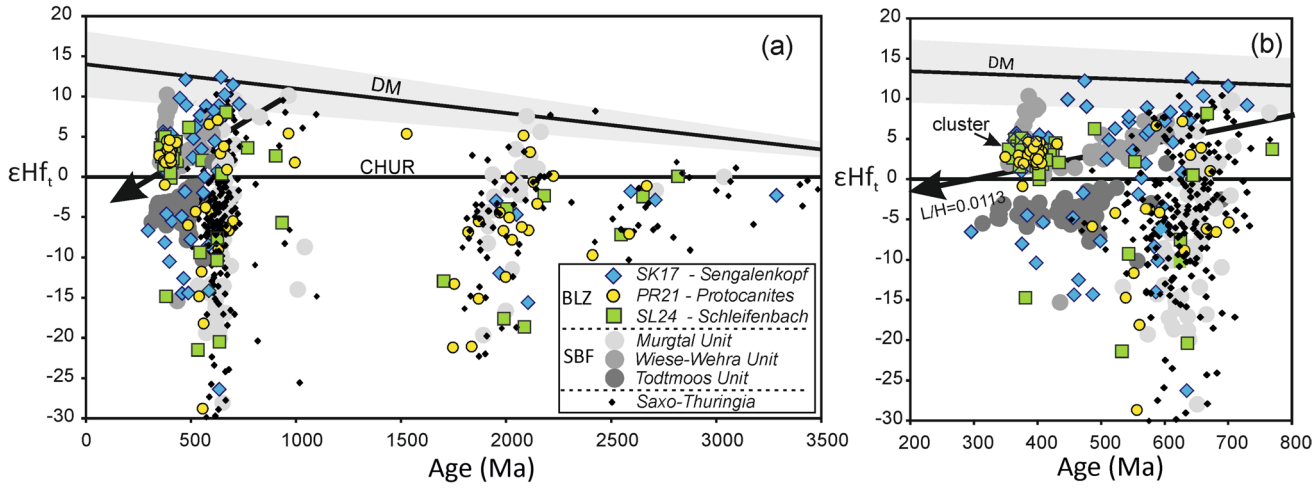

Fig. 7 Age vs. εHf$_t$ diagram showing the data of zircon populations from three formations of the Badenweiler-Lenzkirch Zone (BLZ, this study), compared to data derived from nappe units of the Southern Black Forest Gneiss Complex (SBF, data from Zeh et al. 2023), and from Saxo-Thuringia (data from Bahlburg et al. 2010; Linnemann et al. 2013). **a** all data, **b** only Paleozoic to Neoproterozoic data. Note that zircon grains of all three BLZ units form a cluster with superchondritic εHf$_t$ (+1 to +5) at 370–410 Ma, pointing to a common provenance. The black arrow marks the crustal evolutionary trend (with L/H = ^{176}Lu/.^{177}Hf = 0.0113) derived for the Wiese-Wehra Unit of the Southern Black Forest Gneiss Complex by Zeh et al. (2023). CHUR – chondritic uniform reservoir, DM-depleted mantle evolution according to Chauvel and Blichert-Toft (2001) with 1 sigma limits (grey field)

rounded or disintegrated by peeling, and/or transected by numerous fractures (Fig. 3d, g, h). Furthermore, there are zircon aggregates and crystals intergrown with apatite and/or melt inclusions (Fig. 3e, f). Most zircon grains in all nine samples are non-fragmented or partly fragmented (> 90%), and many of these show perfect euhedral shapes (DOR = 1; up to 45%)—(Table 3). The zircon sizes and size distributions are similar in all samples, as indicated by limited variation in average shape parameters: av. length (l = 86–114 µm), av. width (w = 52–68 µm), and av. aspect ratios (ar = 1.7–1.9; see Fig. 8a-d), as well as by similar grain size distributions, which in all samples are log-normal as indicated by low χ^2 values and SL > 20 (Table 3; ESM-Fig. S1). The degree of roundness is commonly low [DOR(1 to 3) = 43–83%; Table 3]. Zircon grains in samples from the Protocanites Greywacke and Schleifenbachschist formations (Central and Southern units) are commonly more angular (av. DOR = 2.1 to 2.5) compared to those from the six samples from the Sengalenkopfschist Formation (av. DOR = 2.7 to 3.9). The highest DOR is estimated for sample SK352. The zircon typology after Pupin (1980) could be quantified for 39–65% of the zircon grains per sample, except for sample SK352 (only 19%). A wide range of zircon typologies could be distinguished, although seven out of the nine samples display a clear maximum at typology S18 (Fig. 9).

Discussion

Maximum depositional ages

Results of zircon U–Pb dating of the nine samples from the three units of the BLZ yield robust maximum depositional ages (R-MDA's) between 368.0 ± 2.2 and 378.3 ± 3.7 Ma, which for most samples are only slightly older than ages obtained from the youngest zircon grains, ranging from 350 ± 6 Ma to 378 ± 11 Ma (Table 2; Fig. 6). The R-MDA's indicate that the detritus of all BLZ units was deposited during the Late Devonian to Early Carboniferous. For the Protocanites Greywacke Formation (central unit in Fig. 1c), the new data are consistent with the biostratigraphic record (Fig. 2), as well as with Pb-Pb single zircon evaporation ages (371–384 Ma) published by Hegner et al. (2005). Goniatites (*Protocanites*) rarely found in low-strain greywacke domains indicate a Tournaisian age (Korn and Montenari 2023), and conodonts in shale lenses a Late Devonian age (Weyer 1962; Kneidel et al. 1982).

In contrast, acritarchs and chitinozoans rarely found in silty schist layers of the Sengalenkopfschist and Schleifenbachschist formations (northern and southern units) suggest deposition in a marine environment during the

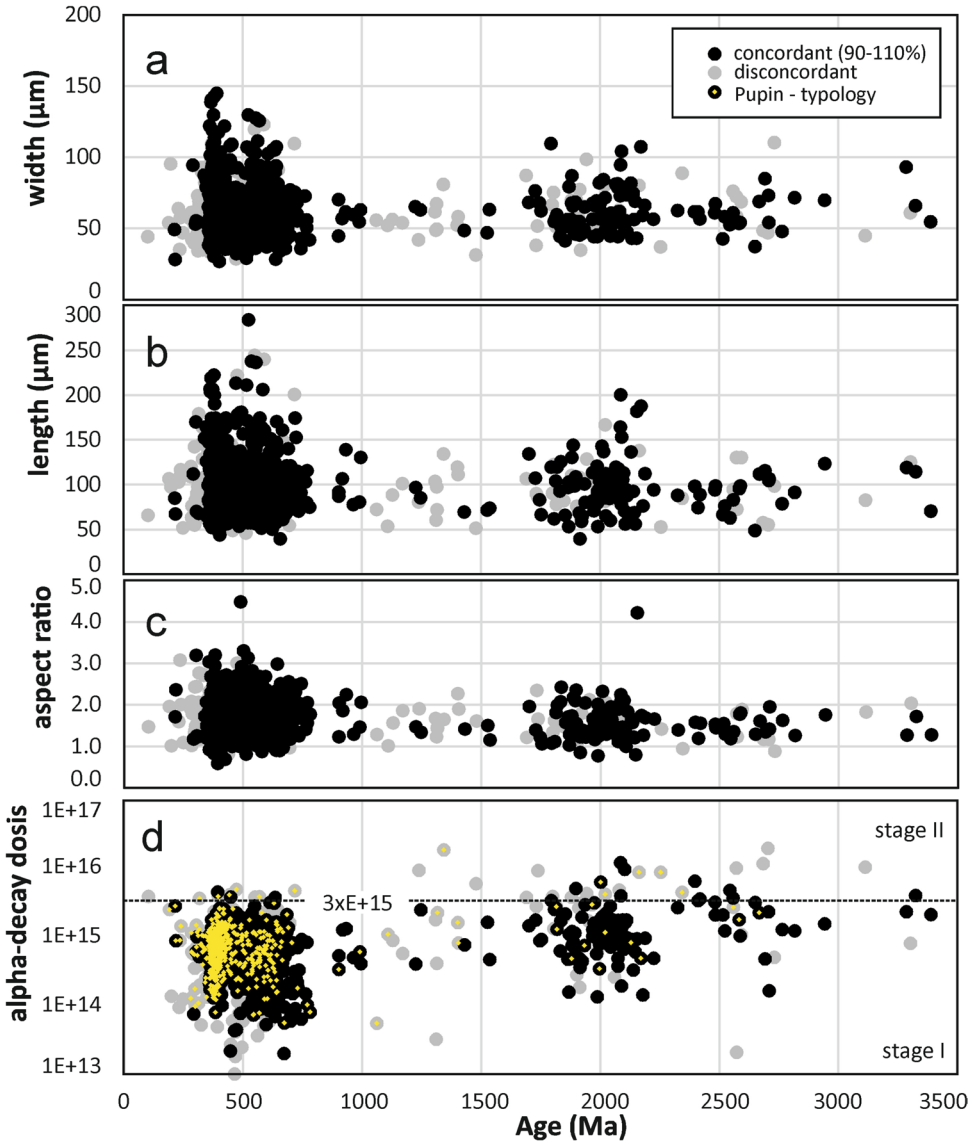

Fig. 8 Variations in zircon shape parameters [**a** width, **b** length, **c** aspect ratio], and in **d** alpha decay doses per mg (present day) with zircon age. The dotted horizontal line in (d) at 3×10^{15} (alpha-decay events per mg) demarcates zircon grains with damage stage I (accumulation of isolated point defects) from stage II (distorted crystalline domains and amorphous tracks) as defined by Murakami et al. (1991). The yellow dots mark zircon grains from which typologies could be estimated

Ordovician to Early Devonian (Hann et al. 1995; Montenari et al. 2000; Vaida et al. 2004). This interpretation, however, is at odds with the detrital zircon age record, which indicates deposition during the Late Devonian to Early Carboniferous. Thus, the results of zircon dating require revision of at least four geological concepts established for the BLZ during previous studies. (1) The fossil record does not reflect the time of greywacke deposition, but rather results from re-deposition of Ordovician to Silurian strata during the Late Devonian to Early Carboniferous. (2) All sedimentary rocks of the BLZ were deposited over less than 30 million years (from 378.3 ± 3.7 Ma to 350 ± 6 Ma) in marine environments immediately prior to Variscan collision at < 345 Ma. (3) Biostratigraphic subdivision of the BLZ into three units, as suggested by the stratigraphic commission of Germany (Hanel et al. 2011) is obsolete, as well as subdivision of the Sengalenkopfschist Formation into a northern and southern belt as introduced by Güldenpfennig (1997). Instead, we suggest the term Badenweiler–Lenzkirch Group comprising all three formations of the BLZ (Sengalenkopfschist, Schleifenbachschist, Protocanites Greywacke formations; Fig. 2). Subdivision into three formations might still be justified considering the different degrees of Variscan structural-metamorphic overprint, and differences in the zircon age spectra (Figs. 4, 5a). The structural-metamorphic overprint is lowest in the Protocanites Greywacke Formation (central unit), and highest in the Sengalenkopfschist Formation (northern unit), in close vicinity to the Rand Granite Nappe, as is indicated by the occurrence of garnet (Fig. 1c). This points to peak metamorphic temperatures of > 450°C (e.g., Hsu 1980; Zeh 2001). (4) Metaconglomerates within the Sengalenkopfschist Formation do not represent dropstones related to Ordovician

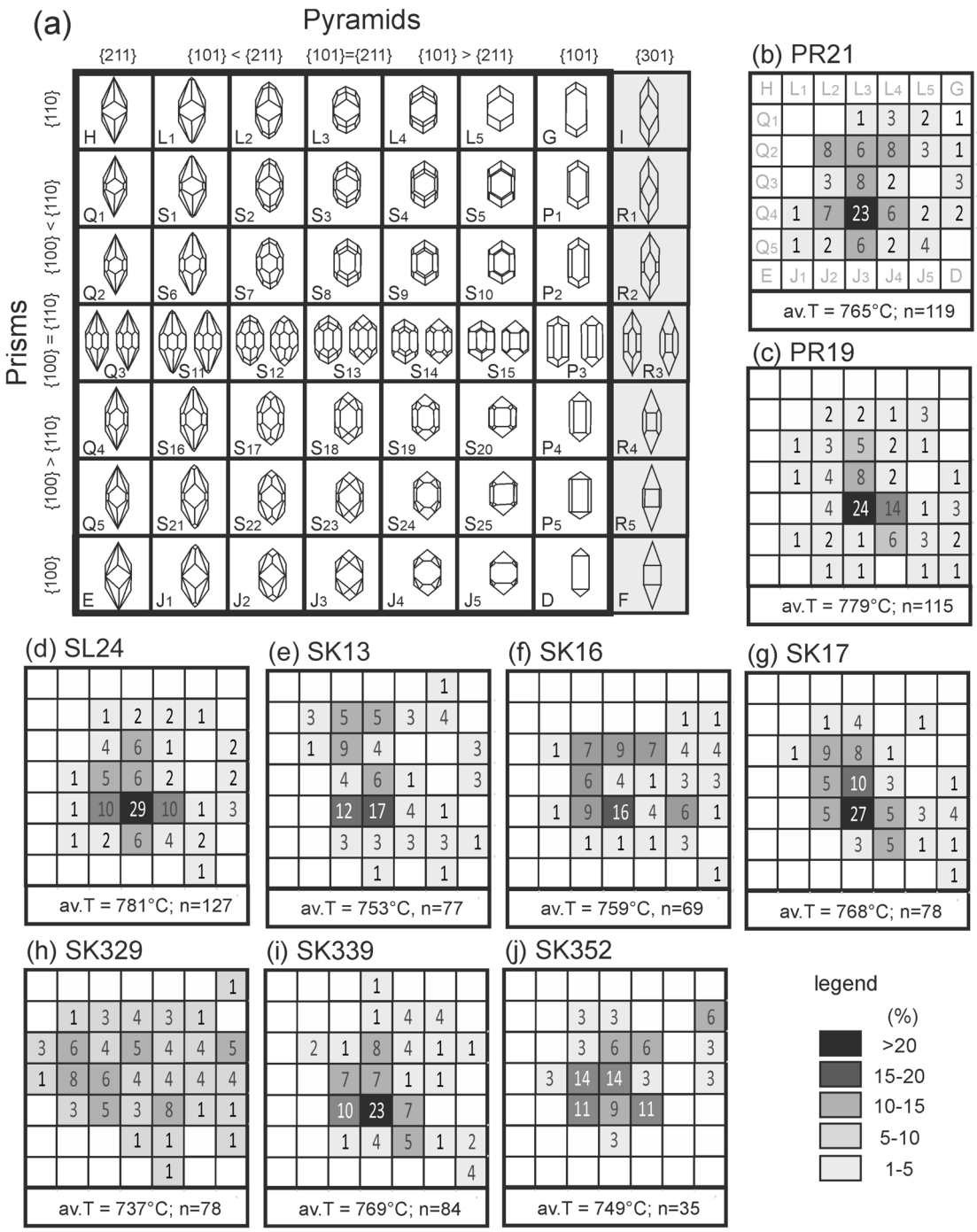

Fig. 9 Topologies of zircon populations in metasedimentary rocks of the Badenweiler-Lenzkirch Zone. **a** Classification scheme according to Pupin (1980). **b** Typology distribution and frequency. Note that most samples show a maximum at typology S18

(Hirnantian) glaciation of Gondwana as suggested by Ziegler and Wimmenauer (2001), but more likely debris flows as submarine channel fills within the greywacke sequence.

Furthermore, it is pertinent to note that the R-MDA's of all Sengalenkopf samples are significantly younger than the single zircon Pb-Pb evaporation age of 393 ± 3 Ma obtained by Hann et al. (2003a) on 3 euhedral zircon grains from a highly sheared metarhyolith within metagreywackes of the quarry Wacht. There are several options to explain this discrepancy. Hann et al. (2003a) already discussed that the origin of the dated metarhyolith is ambiguous, in particular whether it represents a highly sheared rhyolite pebble or a deformed tephra layer. In the light of our new data, and by considering the close spatial relationships of metarhyolith

(Hann et al. (2003a) and metagreywacke (samples SK 13, SK16; this study), the second option appears to be most likely. Alternatively, it is possible that a Late Devonian rhyolite tephra was mixed with surrounding greywacke detritus dominated by euhedral zircon grains with ages of about 393 Ma (see Figs. 3, 4), used for evaporation dating. In addition, reworking of Early Devonian rhyolite ash layers and lava flows during the Late Devonian is possible as well.

Finally, we note that the R-MDA's obtained for the low-grade sedimentary rocks of the BLZ overlap those derived for high-grade paragneisses of the Southern Black Forest Gneiss Complex (Zeh et al. 2023), in particular those of metagreywackes of the Wiese-Wehra Formation (R-MDA = 375 ± 4 Ma) and Todtmoos Formation (R-MDA = 373 ± 3 Ma) – (Fig. 2). This overlap suggests that the BLZ greywackes were deposited contemporaneously or slightly later than those exposed in the Southern Black Forest Gneiss Complex, but experienced a much lower degree of structural-metamorphic overprint during the Variscan orogeny.

Provenance

The zircon age spectra of the nine investigated samples show significant overlap but also differences, as reflected by variable "likeness" values (0.47 to 0.91), and "0–1" values (0.00 to 0.05; Fig. 5a). Low "likeness" values (complementary to high "0–1" values) are reflected in particular by sample SL24 (0.47 to 0.64), mainly due to the absence of zircon grains with ages > 500 Ma, which are common in all other samples, although of different abundance (Fig. 4). The age spectra of most samples display three clusters: (1) a predominant Devonian cluster at 375–410 Ma, (2) an Early Paleozoic to Neoproterozoic cluster at 440–750 Ma (with peaks at 480–500 Ma, 600–620 Ma, and 700–750 Ma), and (3) a Paleoproterozoic cluster at 1800–2200 Ma. Some samples additionally contain a small number of older grains of Paleoproterozoic to Archean ages between 2400 and 3400 Ma, and a minor Tonian-Stenian age cluster at 900–1100 Ma (Fig. 4). Similar age spectra (at $t > 550$ Ma) are reported from metagreywackes of the Murgtal Formation of the Southern Black Forest Gneiss Complex, as well as from many Paleozoic to Neoproterozoic (meta)sedimentary rocks throughout Europe and northern Africa (for compilation see Dörr et al. 2015; and references therein). All these spectra are characterized by a very small number of Tonian-Stenian zircon grains, and an "age gap" between 1.1 and 1.7 Ga, which has first been noted by Zeh et al. (2001). The age spectrum > 500 Ma is commonly interpreted to reflect sediment supply from two major sources: (1) the Avalonian-Cadomian Orogenic Belt (530–750 Ma), and (2) Paleoproterozoic-Archean cratons of Africa (1700–3400 Ma), in addition to (3) minor Neo-Mesoproterozoic sources (900–1100 Ma) located along the margins of proto-Africa (for a detailed discussion see Djerossem et al. 2021). Large variations in εHf_t of the detrital zircon grains of distinct age groups (Paleozoic, Neoproterozoic, Mesoproterozoic, Paleoproterozoic, Archean) from the BLZ indicate variable contribution of crust reworking and new crust addition during different magmatic events (for a detailed compilation and provenance discussion see Zeh et al. 2023). A common feature of all BLZ samples is the predominance of a Devonian zircon population (370–410 Ma) with superchondritic εHf_t ranging from + 1 and + 5 (Fig. 7). This population provides evidence that the greywackes of all three BLZ formations were supplied from similar sources immediately prior to their deposition.

For the Protocanites Greywacke Formation of the BLZ, Hegner et al. (2005) suggested detritus supply from an Andean-type arc system located north of the BLZ, within the Central Gneiss Unit of the Black Forest (Fig. 1b). This interpretation, however, seems to be less likely considering the fact that magmatic rocks of Late Devonian to Early Carboniferous age (370–410 Ma) are completely unknown from the basement units exposed to the north of the BLZ. Orthogneisses within the Central Gneiss Unit only show Cambrian to Early Ordovician protolith ages of c. 500–510 Ma (granitic and tonalitic orthogneisses in the Kinzigtal and Elztal; Chen et al. 2000), or of c. 480 Ma (granites within the Rand Granit Unit; Hann et al. 2003b), and detrital zircon grains from all nappe units show age clusters at 460–520 Ma and 580–610 Ma (Kober et al. 2004), whereas ages between 460 and 370 Ma, which are typical for the BLZ, are very scarce (Fig. 10b, d). Such ages, however, were found abundantly in metagreywackes of the Southern Black Forest Gneiss Complex, in particular in the Wiese-Wehra and Todtmoos units (Zeh et al. 2023). Based on existing datasets, the age spectra derived for the BLZ greywackes can be explained by a mixture of detritus derived from the three nappe units exposed in the Southern Black Forest Gneiss Complex (Wiese-Wehra, Todtmoos, Murgtal). Detrital zircon grains with ages between 370 and 550 overlap those of greywackes from the Wiese-Wehra Unit (superchondritic $\varepsilon Hf_{370\text{-}550\ Ma}$ from 0 to + 10; indicative for juvenile crust formation; Figs. 7, 10), and from the Todtmoos Unit (subchondritic $\varepsilon Hf_{375\text{-}550\ Ma} = -1$ to −15; indicative for crust reworking). Older grains (550–3400 Ma), comprising 5–30% of the BLZ zircon populations, overlap those of the Murgtal Unit (Figs. 7, 10).

Finally, we note that metagreywackes with abundant Devonian to Cambrian zircon grains (370–500 Ma) were also reported from the Böllstein Odenwald (Dörr et al. 2017), located ca. 200 km north of the BLZ, within the Saxothuringian zone. Age-εHf_t spectra similar to those of the Murgtal greywackes were well known from Neoproterozoic to Ordovician greywackes and quartzites of the Saxothuringian zone, e.g., from Thuringia (Gerdes and

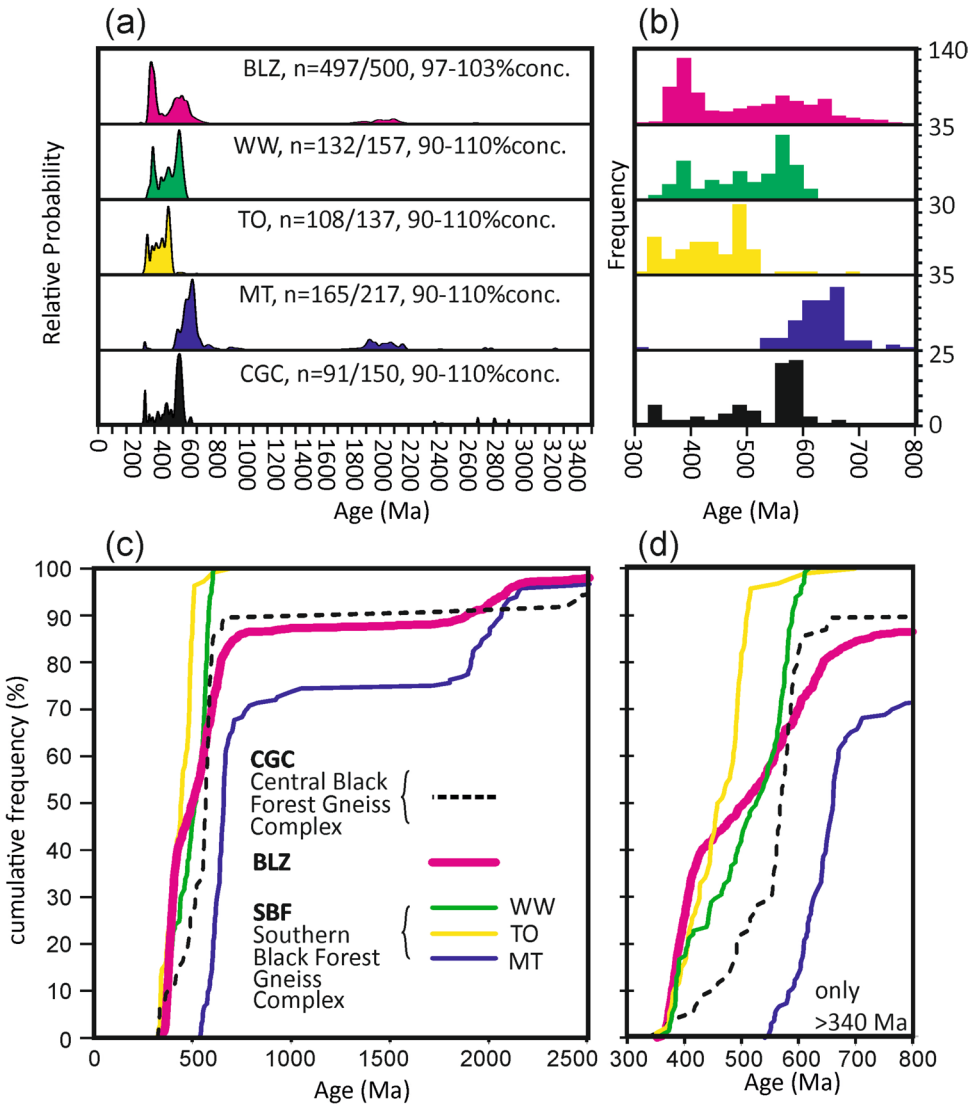

Fig. 10 Comparison of zircon age spectra derived for metasedimentary rocks of the Badenweiler-Lenzkirch Zone (BLZ; this study), for the three nappe units of the Southern Black Forest Gneiss Complex (SBF: WW-Wiese-Wehra, TO-Todtmoos, MT-Murgtal; data from Zeh et al. 2023), and for paragneisses of the Central Black Forest Gneiss Complex (CGC; data from Kober et al. 2004). **a** Kernel density plots, **b** Age vs. frequency plot, **c-d** Age vs. cumulative frequency plots

Zeh 2006; Linnemann et al. 2007, 2013), from the vicinity of the Münchberg Massif (Bahlburg et al. 2010), and the Bergsträsser Odenwald (Dörr and Stein 2019) – (Fig. 7). This overlap shows that sediment sequences of similar provenance were deposited in both the Moldanubian and Saxothuringian realms during the Paleozoic.

Zircon shape and physical parameters

The zircon shape parameters point to similar sources and transport mechanisms for all investigated BLZ greywackes. A proximal magmatic arc source is indicated by two lines of evidence: (1) the large number of detrital zircon grains of euhedral shape in all samples (Table 3), and (2) great overlap in zircon topology (Fig. 9; Table 3), highlighted by similar average zircon formation temperatures (av.T = 737 to 781 °C). The prevailing zircon typologies (S18 and surrounding fields) found in all BLZ samples are common for calc-alkaline magmatic rocks, as has been outlined by Pupin (1980). The large number of zircon grains of euhedral shape further suggests that sediment transport occurred mainly in water-saturated systems (fluvial, marine currents, turbidity flows) and directly from source to sink (perhaps an outer shelf or continental slope environment), without any significant inter-deposition in desert-like (eolian-terrestrial) or shore-line parallel (littoral) environments. These interpretations are in line with the results of previous studies, demonstrating that zircon grains of perfect euhedral shape (DOR = 1) and up to 90 µm diameter (width) can survive fluvial transport of more than 600 km distance (e.g., Zoleikhaei et al. 2016; Zeh and Cabral 2021; Zeh and Wilson 2022), but become quickly rounded (DOR = 4–5) when transported in desert-like (e.g., Garzanti et al. 2012, 2015) or littoral environments (Zeh and Wilson 2022), due to a higher probability of violent grain collisions caused by higher transport

velocity and a missing cushioning effect in the lack of a surface water film.

We further note that zircon typologies could not just be quantified for the youngest detrital zircon grains of Late Devonian age (370–380 Ma), but for most grains with ages < 550 Ma, whereas older grains (550–3400 Ma) are commonly more round (DOR = 3–4), although with numerous exceptions (Figs. 8d). This hints that zircon grains with ages < 550 Ma have been exposed and transported immediately prior to greywacke deposition, whereas older grains (Neoproterozoic, Paleoproterozoic, Archean) were affected by several weathering-transport-deposition cycles. This interpretation is further backed by the observation that younger grains (< 550 Ma) show greater variations in aspect ratios (1.0–3.1), length (50–290 µm) and width (30–150 µm) parameters, compared to older grains (Fig. 8a–c). Finally, it is pertinent to note that most of the investigated zircon grains (> 95%) experienced a relatively low degree of radiogenic damage, as is indicated by alpha decay doses $< 3 \times 10^{-15}$ mg^{-1}, corresponding to the damage-stage I defined by Murakami et al. (1991)—(Fig. 8d). Zircon grains with a higher degree of radiation damage perhaps were destroyed during transport.

Geotectonic implications

The results of this study provide evidence that the BLZ greywackes result from detritus supply from three major sources, equivalent to the nappe units exposed in the Southern Black Forest Gneiss Complex. Results of Zeh et al. (2023) indicate that these units were deposited at different times and in different environments. Greywackes of the Murgtal Unit were deposited during the Ediacarian (ca. 550 Ma) and mainly supplied from the Avalonian-Cadomian Belt (550–800 Ma) and African cratons (1750–3400 Ma). In contrast, greywackes of the Wiese-Wehra and Todtmoos units have Late Devonian maximum depositional ages (ca. 375 Ma) and were derived either from a Late Devonian arc-back arc system ($\varepsilon Hf_t = 0$ to + 10), hosting relics of a Cadomian intra-oceanic arc system initially formed at 610 Ma ($\varepsilon Hf_t = +5$ to + 8), or from a Cambrian to Early Ordovician continental arc (500–480 Ma) dominated by crust reworking ($\varepsilon Hf_t = 0$ to −15). Metarhyolith layers (Hann et al. 2003a), as well as combined zircon age and shape parameters, additionally point to proximal sources and to fast transport from source to sink during the Late Devonian to Early Carboniferous. Taken all information into account, this requires that all three units of the Southern Black Forest Gneiss Complex must have been exposed in close proximity to an oceanic basin successively filled with BLZ greywackes during the Late Devonian to Early Carboniferous (400–350 Ma). A possible model is presented in Fig. 11, which also provides an explanation for the reworking of Ordovician to Silurian marine sediments being the sources for the acritarchs and chitinozoans found in the BLZ greywackes by Vaida et al. (2004). Following greywacke deposition, the oceanic basin

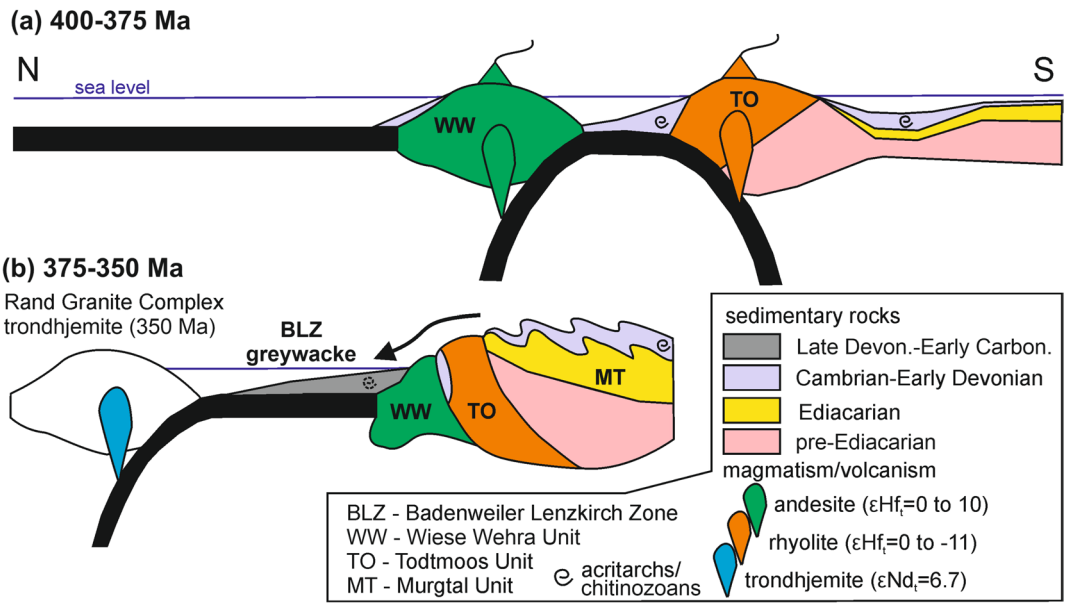

Fig. 11 Model explaining the sources and evolution of the BLZ greywackes between 400 and 350 Ma. **a** Three terranes of different origin (*WW* Wiese-Wehra, *TO* Todtmoos, *MT* Murgtal) approach each other, whereby closing marine basins filled with Ordovician, Silurian to Early Devonian sedimentary rocks. **b** A crustal stack, resulting from the amalgamation of the three terranes, supplies detritus, as well as acritarchs and chitinozoans to an oceanic basin located north of it. This basin was subsequently closed by northward-directed subduction, accompanied by slab melting

became successively closed during the Variscan orogeny, perhaps related to northward-directed subduction, locally accompanied by slab melting (Fig. 11b). This melting resulted in the formation of trondhjemites with juvenile signatures ($\varepsilon Nd_{350Ma} = 6.7$) at 350 Ma, which intruded the Rand Granit Unit located to the north of the BLZ (Hann et al. 2003b).

Conclusions

(1) The protoliths of metagreywackes, quartzites and metaconglomerates of all BLZ units (Sengalenkopfschist, Schleifenbachschist, Protocanites Grauwacke formations) were deposited during the Late Devonian to Early Carboniferous at < 378 Ma.
(2) Early Ordovician to Silurian-Devonian acritarchs and chitinozoans found during previous studies are very likely inherited and supplied from a heterogeneous hinterland, which is indicated by detrital zircon age spectra with pronounced peaks during the Paleozoic-Neoproterozoic (380–400 Ma, 480–500 Ma, 600–620 Ma, 700–750 Ma), and Paleoproterozoic-Archean (between 1700 and 3380 Ma), and very minor peaks during the Tonian-Stenian (950–1100 Ma).
(3) Zircon hafnium isotope data indicate new crust formation from depleted mantle sources during the Late Devonian-Early Carboniferous ($\varepsilon Hf_{375\text{-}430\ Ma}$ up to + 5), in addition to new crust formation and reworking during the Cambro-Ordovician ($\varepsilon Hf_{460\text{-}530\ Ma} = -22$ to + 12), Neoproterozoic ($\varepsilon Hf_{540\text{-}750\ Ma} = -28$ to + 12), Tonian ($\varepsilon Hf_{950\text{-}1100\ Ma} = -6$ to + 5), and Paleoproterozoic ($\varepsilon Hf_{1700\text{-}2200\ Ma} = -22$ to + 5).
(4) The finding of abundant detrital zircon grains of euhedral shape and with similar typologies in all BLZ samples suggest sediment supply from a proximal hinterland, and transport in water-saturated media (fluvial systems, shallow marine currents, turbidity flows).
(5) Compilation of age-Hf isotope data further suggest that all BLZ greywackes were supplied from three major sources, equivalent to the nappe units exposed in the southern Black Forest Gneiss Complex (Wiese-Wehra, Todtmoos, Murgtal).

Supplementary Information The online version contains supplementary material available at https://doi.org/10.1007/s00531-025-02532-z.

Acknowledgements AZ and MH are grateful to Deutsche Forschungsgemeinschaft (DFG grants ZE 424/17-1; Hi 643/25-1) for financial support, and Horst Hann and Hubert Zedler for guidance in the field. Furthermore, many thanks to Ricardo Arenas and Wolfgang Siebel for constructive reviews, and to Ulrich Riller and Guido Meinhold for editorial handling.

Author contributions Armin Zeh: conceptualization, methodology, U–Pb dating, formal analysis, investigation, writing—original draft, funding acquisition. Matthias Hinderer: field work, sampling, writing, editing, funding acquisition. Calvin Diehl: field work, sampling, writing. Axel Gerdes: methodology, Lu–Hf isotope, software.

Funding Open Access funding enabled and organized by Projekt DEAL.

Data availability All data are presented in supplementary information.

Declarations

Conflict of interest The authors declare that they have no known competing financial interests or personal relationships that could have appeared to influence the work reported in this paper.

References

Altherr R, Henjes-Kunst F, Langer C, Otto J (1999) Interaction between crustal-derived felsic and mantle-derived mafic magmas in the Oberkirch Pluton (European Variscides, Schwarzwald, Germany). Contrib Miner Petrol 137:304–322. https://doi.org/10.1007/s004100050552

Altherr R, Holl A, Hegner E, Langer C, Kreuzer H (2000) High-potassium, calc-alkaline I-type plutonism in the European Variscides: Northern Vosges (France) and Northern Schwarzwald (Germany). Lithos 50:51–73. https://doi.org/10.1016/S0024-4937(99)00052-3

Altherr R, Hanel M, Schwarz WH, Wimmenauer W (2019) Petrology and U-Pb zircon age of the Variscan porphyroclastic Rand Granite at the southeastern margin of the Central Schwarzwald Gneiss Complex (Germany). Int J Earth Sci (Geol Rundsch) 108:1879–1895. https://doi.org/10.1007/s00531-019-01738-2

Andersen T, Kristoffersen M, Elburg MA (2018) Visualizing, interpreting and comparing detrital zircon age and Hf isotope data in basin analysis – a graphical approach. Basin Res 30:132–147. https://doi.org/10.1111/bre.12245

Bahlburg H, Vervoort JD, DuFrane SA (2010) Plate tectonic significance of Middle Cambrian and Ordovician siliciclastic rocks of the Bavarian facies, Armorican terrane assemblage, Germany — U-Pb and Hf isotope evidence from detrital zircons. Gondwana Res 17:223–235. https://doi.org/10.1016/j.gr.2009.11.007

Bouvier A, Vervoort JD, Patchett PJ (2008) The Lu-Hf and Sm-Nd isotopic composition of CHUR: constraints from unequilibrated chondrites and implications for the bulk composition of terrestrial planets. Earth Planet Sci Lett 273:48–57. https://doi.org/10.1016/j.epsl.2008.06.010

Chauvel C, Blichert-Toft J (2001) A hafnium isotope and trace element perspective on melting of the depleted mantle. Earth Planet

Sci Lett 190:137–151. https://doi.org/10.1016/S0012-821X(01)00379-X

Chen F, Hegner E, Todt W (2000) Zircon ages and Nd isotopic and chemical compositions of orthogneisses from the Black Forest, Germany: evidence for a Cambrian magmatic arc. Int J Earth Sci (Geol Rundsch) 88:791–802. https://doi.org/10.1007/s005310050306

Djerossem F, Zeh A, Isseini M, Vanderhaeghe O, Berger J, Ganne J (2021) U-Pb-Hf isotopic systematics of zircons from granites and metasediments of southern Ouaddai (Chad), implications for crustal evolution and provenance in the Central Africa orogenic belt. Precam Res 361:106233. https://doi.org/10.1016/j.precamres.2021.106233

Dörr W, Stein E (2019) Precambrian basement in the Rheic suture zone of the Central European Variscides (Odenwald). Int J Earth Sci (Geol Rundsch) 108:1937–1957. https://doi.org/10.1007/s00531-019-01741-7

Dörr W, Zulauf G, Gerdes A, Lahaye Y, Kowalczyk G (2015) A hidden Tonian basement in the eastern Mediterranean: age constraints from U-Pb data of magmatic and detrital zircons of the External Hellenides (Crete and Peloponnesus). Precam Res 258:83–108. https://doi.org/10.1016/j.precamres.2014.12.015

Dörr W, Zulauf G, Gerdes A, Loeckle F (2017) Provenance of upper Devonian clastic (meta)sediments of the Böllstein Odenwald (Mid-German-Crystalline-Zone, Variscides). Int J Earth Sci (Geol Rundsch) 106:2927–2943. https://doi.org/10.1007/s00531-017-1473-x

Eisbacher GH, Lüschen E, Wickert F (1989) Crustal-scale thrusting and extension in the Hercynian Schwarzwald and Vosges, central Europe. Tectonics 8:1–21. https://doi.org/10.1029/TC008i001p00001

Finger F, Riegler G (2022) Is there an upper Devonian rift zone under the northern front of the Alps separating East and West Armorican crustal segments? Geol Carpath 73(3):181–185. https://doi.org/10.31577/GeolCarp.73.3.1

Flöttmann T, Kleinschmidt G (1989) Structural and basement evolution in the central Schwarzwald gneiss complex. In: Emmermann R, Wohlenberg J (eds) The German Continental Deep Drilling Program (KTB). Springer, Berlin, pp 266–275

Franke W, Cocks LRM, Torsvik TH (2017) The palaeozoic variscan oceans revisited. Gondwana Res 48:257–284. https://doi.org/10.1016/j.gr.2017.03.005

Garzanti E, Andò S, Vezzoli G, Lustrino M, Boni M, Vermeesch P (2012) Petrology of the Namib Sand Sea: long-distance transport and compositional variability in the wind-displaced Orange Delta. Earth-Sci Rev 11:173–189. https://doi.org/10.1016/j.earscirev.2012.02.008

Garzanti E, Resentini A, Andò S, Vezzoli G, Pereira A, Vermeesch P (2015) Physical controls on sand composition and relative durability of detrital minerals during ultra-long distance littoral and aeolian transport (Namibia and southern Angola). Sedimentology 62:971–996. https://doi.org/10.1111/sed.12169

Gerdes A, Zeh A (2006) Combined U-Pb and Hf isotope LA-(MC-)ICP-MS analyses of detrital zircons: comparison with SHRIMP and new constraints for the provenance and age of an Armorican metasediment in Central Germany. Earth Planet Sci Lett 249:47–61. https://doi.org/10.1016/j.epsl.2006.06.039

Gerdes A, Zeh A (2009) Zircon formation versus zircon alteration – new insights from combined U-Pb and Lu-Hf in-situ LA-ICP-MS analyses, and consequences for the interpretation of Archean zircon from the Limpopo Belt. Chem Geol 261:230–243. https://doi.org/10.1016/j.chemgeo.2008.03.005

Güldenpfenning M (1997) Geologische Neuaufnahme der Zone von Badenweiler–Lenzkirch (Südschwarzwald) unter besonderer Berücksichtigung unterkarbonischer Vulkanite und Grauwacken. Tübinger Geowiss Abh 32:120 pp.

Haas I, Eichinger S, Haller D, Fritz H, Nievoll J, Mandl M, Hippler D, Hauzenberger C (2020) Gondwana fragments in the Eastern Alps: a travel story from U/Pb zircon data. Gondwana Res 77:204–222. https://doi.org/10.1016/j.gr.2019.07.015

Hanel M, Wimmenauer W (1990) Petrographische Indizien für einen Deckenbau im Kristallin des Schwarzwaldes. Eur J Min 2:89

Hanel M, Lippolt HJ, Kober B, Wimmenauer W (1993) Lower Carboniferous granulites in the Schwarzwald basement near Hohengeroldseck (SW Germany). Naturwissenschaften 80:25–28. https://doi.org/10.1007/BF01139753

Hanel M, Kesler G, Sawatzki G, Wimmenauer W (2001) Schwarzwald (15). In: Steininger F (ed) Stratigraphische Kommission Deutschland, Stratigraphie von Deutschland II Ordovizium Kambrium Vendium Riphäikum. Courier Forschungsinstitute Senckenberg, Frankfurt, pp 13–181

Hann HP, Sawatzki G (1998) Deckenbau und Sedimentationsalter im Grundgebirge des Südschwarzwaldes/SW-Deutschland. Z Dtsch Geol Ges 149:183–195. https://doi.org/10.1127/zdgg/149/1998/183

Hann HP, Sawatzki G, Vaida M (1995) Acritarchen und Chitinozoen des Ordoviziums aus metamorphen Grauwacken der Zone von Badenweiler-Lenzkirch, Schwarzwald, SW-Deutschland. N Jb Geol Paläont, Mh 6:375–383. https://doi.org/10.1127/njgpm/1995/1995/375

Hann HP, Chen F, Zedler H, Sawatzki G (2003a) Zircon ages and geochemistry of metavolcanic layers from the northern Badenweiler-Lenzkirch Zone (southern Schwarzwald, Germany). N Jb Geol Paläont 230:451–469

Hann HP, Chen F, Zedler H, Frisch W, Loeschke J (2003b) The rand granite in the southern Schwarzwald and its geodynamic significance in the Variscan belt of SW Germany. Int J Earth Sci (Geol Rundsch) 92:821–842. https://doi.org/10.1007/s00531-003-0361-8

Hegner E, Chen F, Hann HP (2001) Chronology of basin closure and thrusting in the internal zone of the Variscan belt in the Schwarzwald, Germany: evidence from zircon ages, trace element geochemistry, and Nd isotopic data. Tectonophysics 332:169–184. https://doi.org/10.1016/S0040-1951(00)00254-7

Hegner E, Gruler M, Hann HP, Chen F, Güldenpfennig M (2005) Testing tectonic models with geochemical provenance parameters in greywacke. J Geol Soc London 162:87–96. https://doi.org/10.1144/0016-764904-029

Hsu LC (1980) Hydration and phase relations of grossular-spessartine garnets at P_{H2O}=2 kb. Contrib Miner Petrol 71:407–415. https://doi.org/10.1007/BF00374712

Kalt A, Altherr R (1996) Metamorphic evolution of garnet-spinel peridotites from the Variscan Schwarzwald (Germany). Geol Rundsch 85:211–224. https://doi.org/10.1007/BF02422229

Kalt A, Altherr R, Hanel M (2000) The variscan basement of the Schwarzwald. Eur J Miner 12:1–43

Kneidl V, Krebs W, Maass R (1982) Über Conodontenfunde im Oberdevon von Tunau (Südschwarzwald). N Jb Geol Paläont Mh 1982:25–35. https://doi.org/10.1127/njgpm/1982/1982/25

Kober B, Kalt A, Hanel M, Pidgeon RT (2004) Shrimp dating of zircons from high-grade metasediments of the Schwarzwald/SW-Germany and implications for the evolution of the Moldanubian basement. Contrib Mineral Petrol 147:330–345. https://doi.org/10.1007/s00410-004-0560-8

Korn D, Montenari M (2023) Re-assessment of ammonoid specimens from the Early Carboniferous Protocanites Beds of the Badenweiler-Lenzkirch Zone (Schwarzwald, Central Variscan Belt): age constraints for a lithostratigraphic key bed. PalZ 97:761–768. https://doi.org/10.1007/s12542-021-00577-4

Kossmat F (1927) Gliederung des varistischen Gebirgsbaues. Abh Saechs Geol Landesamtes 1:1–39

Kroner U, Romer RL (2013) Two plates — many subduction zones: the Variscan orogeny reconsidered. Gondwana Res 24:298–329. https://doi.org/10.1016/j.gr.2013.03.001

Kroner U, Mansy J-L, Mazur S, Aleksandrowski P, Hann HP, Huckriede H, Lacquement F, Lamarche J, Ledru P, Pharaoh TC, Zedler H, Zeh A, Zulauf G (2008) Variscan tectonics. In: McCann T (ed) The Geology of Central Europe: Precambrian and Palaeozic, vol 1. Geology Society of London, pp 599–665

Linnemann U, Gehmlich M, Tichomirowa M, Buschmann B, Nasdala L, Jonas P, Lützner H, Bombach K (2000) From Cadomian subduction to early Palaeozoic rifting: the evolution of Saxo-Thuringia at the margin of Gondwana in the light of single zircon geochronology and basin development (Central European Variscides, Germany). Geol Soc London Spec Publ 179:131–153. https://doi.org/10.1144/GSL.SP.2000.179.01.10

Linnemann U, McNaughton NJ, Romer RL, Gehmlich M, Drost K, Tonk C (2004) West African provenance for Saxo-Thuringia (Bohemian Massif): did Armorica ever leave pre-Pangean Gondwana? – U/Pb-SHRIMP zircon evidence and the Nd-isotopic record. Int J Earth Sci (Geol Rundsch) 93:683–705. https://doi.org/10.1007/s00531-004-0413-8

Linnemann U, Gerdes A, Drost K, Buschmann B (2007) The continuum between Cadomian Orogenesis and opening of the Rheic Ocean: constraints from LA–ICP–MS U-Pb zircon dating and analysis of plate-tectonic setting (Saxo-Thuringian zone, NE Bohemian massif, Germany). In: Linnemann U, Nance RD, Kraft P, Zulauf G (eds) The evolution of the Rheic Ocean: From Avalonian-Cadomian Active Margin to Alleghenian-Variscan Collision. Geological Society of America, pp 61–96

Linnemann U, Gerdes A, Mandy Hofmann M, Marko L (2013) The Cadomian Orogen: Neoproterozoic to Early Cambrian crustal growth and orogenic zoning along the periphery of the West African Craton—Constraints from U-Pb zircon ages and Hf isotopes (Schwarzburg Antiform, Germany). Precam Res 244:236–327. https://doi.org/10.1016/j.precamres.2013.08.007

Ludwig KR (2012) User's Manual for Isoplot 3.75: a geochronological toolkit for microsoft excel. Berkeley Geochronol Center Spec Pub 5:75

Marschall HR, Kalt A, Hanel M (2003) P-T evolution of a Variscan lower-crustal segment: a study of granulites from the Schwarzwald, Germany. J Petrol 44:227–253. https://doi.org/10.1093/petrology/44.2.227

Montenari M, Servais T (2000) Early palaeozoic (late Cambrian-early Ordovician) acritarchs from the metasedimentary Baden-Baden-Gaggenau zone (Schwarzwald), SW Germany). Rev Palaeobot Palynol 113:73–85. https://doi.org/10.1016/S0034-6667(00)00053-1

Montenari M, Servais T, Paris F (2000) Palynological dating (acritarchs and chitinozoans) of lower Paleozoic phyllites from the Black Forest/southwestern Germany. Compt Rend Acad Sci Ser IIA Earth Planet Sci 330:493–499. https://doi.org/10.1016/S1251-8050(00)00182-8

Murakami T, Chakoumakos BC, Ewing RC, Lumpkin GR, Weber WJ (1991) Alpha-decay event damage in zircon. Am Mineral 76:1510–1532

Neubauer F, Liu Y, Dong Y, Chang R, Genser J, Yuan S (2022) Prealpine tectonic evolution of the Eastern Alps: from Prototethys to Paleotethys. Earth Sci Rev 226:103923. https://doi.org/10.1016/j.earscirev.2022.103923

Pupin JP (1980) Zircon and granite petrology. Contrib Mineral Petrol 73:207–220. https://doi.org/10.1007/BF00381441

Röhr C (1990) Die Genese der Leptinite und Paragneise zwischen Nordrach und Gengenbach im mittleren Schwarzwald. Frankfurter Geowiss Arbeiten Serie C 11:1–59

Satkoski AM, Wilkinson BH, Hietpas JH, Samson SD (2013) Likeness among detrital zircon populations—an approach to the comparison of age frequency data in time and space. Geol Soc Am Bull 125:1783–1799. https://doi.org/10.1130/B30888.1

Sawatzki G, Hann HP (2003) Erläuterungen zur Geologischen Karte der Badenweiler-Lenzkirch-Zone im Südschwarzwald (1:50.000) mit Hinweisen für Exkursionen.- Landesamt für Geologie Rohstoffe und Bergbau Baden-Württemberg, Freiburg im Breisgau, p 1–182, Freiburg i. Br.

Schaltegger U (2000) U-Pb geochronology of the Southern Black Forest Batholith (Central Variscan Belt): timing of exhumation and granite emplacement. Int J Earth Sci (Geol Rundsch) 88:814–828. https://doi.org/10.1007/s005310050308

Scherer E, Münker C, Mezger K (2001) Calibration of the lutetium-hafnium clock. Science 293:683–687. https://doi.org/10.1126/science.1061372

Schleicher H (1994) Collision-type granitic melts in the context of thrust tectonics and uplift history (Triberg granite complex, Schwarzwald, Germany). N Jb Mineral Abh 166:211–237

Schönenberg R, Neugebauer J (1997) Einführung in die Geologie Europas. Rombach Verlag, Freiburg in Breisgau, p 385

Sebert M, Wimmenauer W (1992) Metagabbros and metaanorthosites in the Southern Black Forest. Jahresh Geol Landesamtes Baden-Württemberg 34:167–212

Sircombe KN (2004) Agedisplay: an EXCEL workbook to evaluate and display univariate geochronological data using binned frequency histograms and probability density distributions. Comput Geosci 30:21–31. https://doi.org/10.1016/j.cageo.2003.09.006

Söderlund U, Patchett PJ, Vervoort JD, Isachsen CE (2004) The ^{176}Lu decay constant determined by Lu-Hf and U-Pb isotope systematics of Precambrian mafic intrusions. Earth Planet Sci Lett 219:311–324. https://doi.org/10.1016/S0012-821X(04)00012-3

Stacey JS, Kramers JD (1975) Approximation of terrestrial lead isotope evolution by a two-stage model. Earth Planet Sci Lett 26:207–221. https://doi.org/10.1016/0012-821X(75)90088-6

Stampfli GM, von Raumer JF, Borel GD (2002) Paleozoic evolution of pre-Variscan terranes: From Gondwana to the Variscan collision. In: Martínez Catalán JR, Hatcher RD Jr, Arenas R, Díaz García F (eds) Variscan-Appalachian dynamics: The building of the late Paleozoic basement. Geological Society of America, Boulder Colorado, pp 263–280

Tait JA, Bachtadse V, Franke W, Soffel HC (1997) Geodynamic evolution of the European Variscan fold belt: paleomagnetic and geological constaints. Geol Rundsch 86:585–598. https://doi.org/10.1007/s005310050165

Taylor SR, McLennan SM (1985) The continental crust: its composition and evolution. Blackwell, Oxford, p 312

Vaida M, Hann HP, Sawatzki G, Frisch W (2004) Ordovician and Silurian protolith ages of metamorphosed clastic sedimentary rocks from the southern Schwarzwald, SW Germany: a palynological study and its bearing on the early Palaeozoic geotectonic evolution. Geol Mag 141:629–643. https://doi.org/10.1017/S0016756804009641

von Raumer JF, Stampfli GM, Borel G, Bussy F (2002) Organization of pre-Variscan basement areas at the north-Gondwanan margin. Int J Earth Sci (Geol Rundsch) 91:35–52. https://doi.org/10.1007/s005310100200

von Raumer JF, Bussy F, Schaltegger U, Schulz B, Stampfli GM (2013) Pre-mesozoic alpine basements—their place in the european paleozoic framework. Geol Soc America Bull 125:89–108. https://doi.org/10.1130/B30654.1

Wedepohl KH (1995) The composition of the continental crust. Geochim Cosmochim Acta 59:1217–1232. https://doi.org/10.1016/0016-7037(95)00038-2

Weyer D (1962) Zwei Oberdevon-Faunen von Schönau im Südschwarzwald. Geologie 11:384–396

Wickert F, Altherr R, Deutsch M (1990) Polyphase variscan tectonics and metamorphism along a segment of the

Saxothuringian-Moldanubian boundary: the Baden-Baden zone, northern Schwarzwald (FRG). Geol Rundsch 79:627–647

Wimmenauer W (1988) Precambrian in the horst mountains of the Rhine graben area. In: Zoubek V (ed) Precambrian in younger fold belts European Variscides the Carpathians and Balkans. Wiley, Chichester, pp 381–408

Woodhead JD, Hergt JM (2005) A preliminary appraisal of seven natural zircon reference materials for in situ Hf isotope determination. Geostand Geoanal Res 29:183–195. https://doi.org/10.1111/j.1751-908X.2005.tb00891.x

Žák J, Sláma J (2017) How far did the Cadomian 'terranes' travel from Gondwana during early Palaeozoic? A critical reappraisal based on detrital zircon geochronology. Int Geol Rev 60:319–338. https://doi.org/10.1080/00206814.2017.1334599

Žák J, Sláma J, Syahputra R, Nance RD (2023) Dynamics of cambro-ordovician rifting of the northern margin of Gondwana as revealed by the timing of subsidence and magmatism in rift-related basins. Int Geol Rev 66:1956–1970. https://doi.org/10.1080/00206814.2023.2172619

Zeh A (2001) Inference of a detailed P-T path from P-T pseudosections using metapelitic rocks of variable composition from a single outcrop, Shackleton Range, Antarctica. J Metamorph Geol 19:329–350. https://doi.org/10.1046/j.0263-4929.2000.00314.x

Zeh A, Cabral AR (2021) Combining detrital zircon shape and U-Pb–Hf-isotope analyses for provenance studies – an example from the Aquiri region, Amazon Craton, Brazil. Precam Res 364:106343. https://doi.org/10.1016/j.precamres.2021.106343

Zeh A, Wilson AH (2022) U-Pb-Hf isotopes and shape parameters of zircon from the Mozaan Group (South Africa) with implications for depositional ages, provenance and Witwatersrand – Pongola Supergroup correlations. Precam Res 368:106500. https://doi.org/10.1016/j.precamres.2021.106500

Zeh A, Brätz H, Millar IL, Williams IS (2001) A combined zircon SHRIMP and Sm-Nd isotope study on high-grade paragneisses from the Mid-German Crystalline Rise: evidence for northern Gondwanan and Grenvillian provenance. J Geol Soc London 158:983–994. https://doi.org/10.1144/0016-764900-186

Zeh A, Zimmermann M, Albert R, Drüppel K, Gerdes A (2023) Zircon U-Pb-Hf isotope systematics of southern Black Forest gneiss units (Germany) – implications for the pre-Variscan evolution of Central Europe. Gondwana Res 128:351–367. https://doi.org/10.1016/j.gr.2023.11.008

Ziegler P, Wimmenauer W (2001) Possible glacio-marine diamictites in Lower Paleozoic series of the Southern Black Forest (Germany): implications for the Gondwana/Laurussia puzzle. N Jb Geol Palaont Mh 8:500–512. https://doi.org/10.1127/njgpm/2001/2001/500

Zoleikhaei Y, Frei D, Morton A, Zamanzadeh SM (2016) Roundness of heavy minerals (zircon and apatite) as a provenance tool for unravelling recycling: a case study from the Sefidrud and Sarbaz rivers in N and SE Iran. Sediment Geol 342:106–117. https://doi.org/10.1016/j.sedgeo.2016.06.016